

Gas and Liquid Flow in Shale*

Farzam Javadpour¹

Search and Discovery Article #41780 (2016)**

Posted March 28, 2016

*Adapted from oral presentation at Geoscience Technology Workshop, Unconventionals Update, Austin, Texas, November 3, 2015

**Datapages © 2016 Serial rights given by author. For all other rights contact author directly.

¹University of Texas at Austin, Austin, TX, USA (farzam.javadpour@beg.utexas.edu)

Abstract

Shale gas strata, important energy supplies in North America, are projected to become important as well in Europe, Latin America, and Asia in the near future. Gas and oil production from these fine-grained reservoirs is technically challenging, however fluid flow as observed in field is much higher than predictions based on conventional models (Darcy's equation). Clear understanding of gas/liquid flow in these natural, fine-grained, porous systems is necessary in making capital investments, as well as in making field-development decisions by governments and major oil companies. This talk presents detailed discussion of gas and liquid flow in tiny pores (nanometer scale). Novel research methods and challenges for reserve estimation and permeability predictions will also be presented.

Selected References

Darabi, H., A. Ettehad, F. Javadpour, and K. Sepehrnoori, 2012, Gas flow in ultra-tight shale strata: Journal of Fluid Mechanics, v. 710, p. 641-658.

Etminan, S.R., F. Javadpour, B.B. Maini, and Z. Chen, 2014, Measurement of gas storage processes in shale and of the molecular diffusion coefficient in kerogen: International Journal of Coal Geology, v. 123, p. 10-19

Freeman, C.M., G.J. Moridis, G.E. Michael, and T.A. Blasingame, 2012, Measurement, Modeling, and Diagnostics of Flowing Gas Composition Changes in Shale Gas Wells: SPE Paper 153391, Proceedings, SPE Latin American and Caribbean Petroleum Engineering Conference, Mexico City, Mexico, 16-18 April 2012.

Gale, J.F.W., R.M. Reed, and J. Holder, 2007, Natural fractures in the Barnett Shale and their importance for hydraulic fracture treatments: AAPG Bulletin, v. 91/4, p. 603-622.

Hosseini, S.A., F. Javadpour, and G.E. Michael, 2015, Novel Analytical Core-Sample Analysis Indicates Higher Gas Content in Shale-Gas Reservoirs: Society of Petroleum Engineers, doi:10.2118/174549-PA.

Javadpour, F., 2007, Bubble breakup in porous media: Journal of Canadian Petroleum Technology, v. 46/8, p. 26-33.

Javadpour, F., 2009, Nanopores and apparent permeability of gas flow in mudrocks (shales and siltstone): Journal of Canadian Petroleum Technology, v. 48/8, p. 16-21.

Javadpour, F., M.M. Farshi, and M. Amrein, 2012, Atomic-force microscopy: a new tool for gas-shale characterization: Journal of Canadian Petroleum Technology, v. 51/4, p. 236-243.

Javadpour, F., M. McClure, and M.E. Naraghi, 2015, Slip-corrected liquid permeability and its effect on hydraulic fracturing and fluid loss in shale: Fuel, v. 160, p. 549-559.

Loucks, R.G., R.M. Reed, S.C. Ruppel, and U. Hammes, 2012, Spectrum of pore types and networks in mudrocks and a descriptive classification for matrix-related mudrock pores: AAPG Bulletin, v. 96/6, p. 1071-1098.

Mehmani, A., M. Prodanović, and F. Javadpour, 2013, Multiscale, multiphysics network modeling of shale matrix gas flows: Transport in Porous Media, v. 99/2, p. 377-390.

Naraghi, M.E., and F. Javadpour, 2015, A stochastic permeability model for the shale-gas systems: International Journal of Coal Geology, v. 140, p. 111-124.

Rezaveisi, M., F. Javadpour, and K. Sepehrnoori, 2014, Modeling chromatographic separation of produced gas in shale wells: International Journal of Coal Geology, v. 121, p. 110-122.

Roy, S., R. Raju, H.F. Chuang, B.A. Cruden, and M. Meyyappan, 2003, Modeling gas flow through microchannels and nanopores: J. Appl. Phys. v. 93, <http://dx.doi.org/10.1063/1.1559936>

Waechter, N.B., G.L. Hampton III, S.D. Schwochow, and J.P. Seidle, 2004, Accurate gas content analysis improves coalbed gas resource estimation: careful acquisition, handling and analysis of coal samples in the field and in the laboratory help pin down elusive “lost gas” for resource calculations: World Oil, v. 225/8, p. 47-51.

Gas and Liquid Flow in Shale

Farzam Javadpour

11/03/2015

**Unconventional Update
AAPG Geoscience Technology Workshop**

Outline

- Brief introduction of nanophysics
- Shale system
 - Gas-in-place and transport
 - Diffusion in kerogenic material
 - Lost gas
 - Stochastic permeability model
 - In-situ gas chromatography separation
 - Liquid flow and fracture fluid loss

What is nanoscience?

Nano refers to one-billionth of something (10^{-9})

e.g., nanograms, nanoliters, nanometers

Diameter of a hair string: 75,000 nm

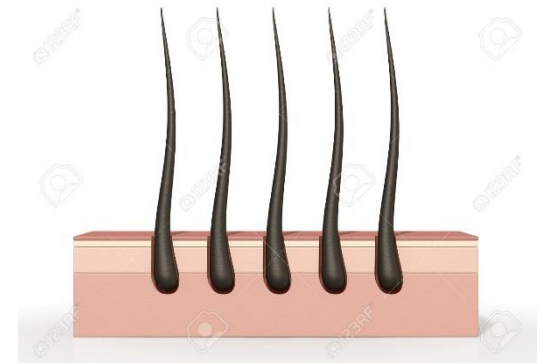
Pores in sandstone: 50,000 nm

Red blood cell: 7,000 nm

Pores in shale: 10 nm

Water molecule: 0.3 nm

Nanoscience is the study of structures and materials on the scale of nanometers.



Nanoscale research needs

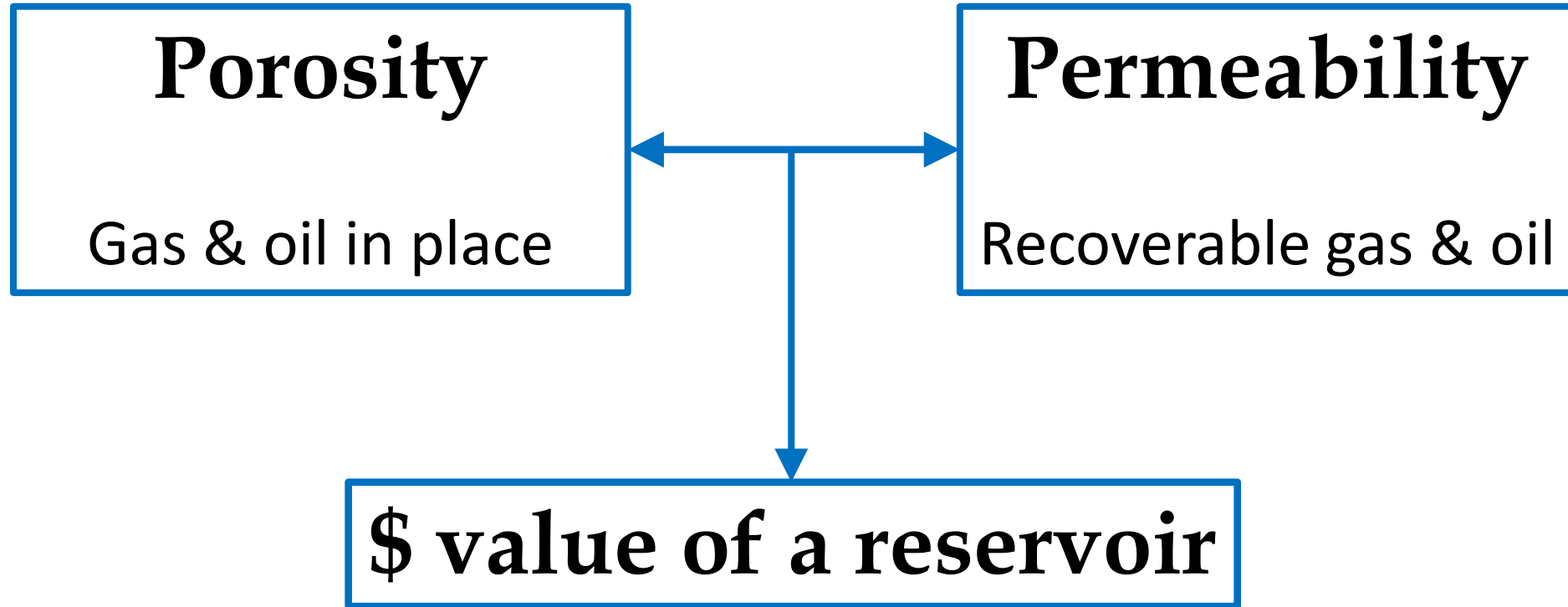
- Sophisticated measuring devices
- Deep understanding of fundamental physics.
Different from continuum physics

Applications & our interest

Natural nanosystems

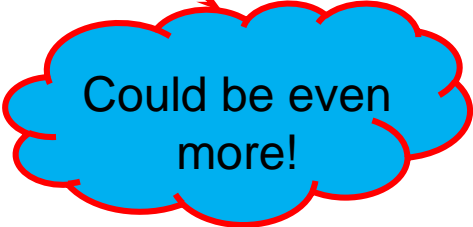
Shale plays

Applications in shale plays



Interesting statistics

EIA report	2011	2013
Recoverable shale gas resources (Tcf)	6,622	7,299
Recoverable shale/tight oil (B bbl)	32	345



Could be even more!

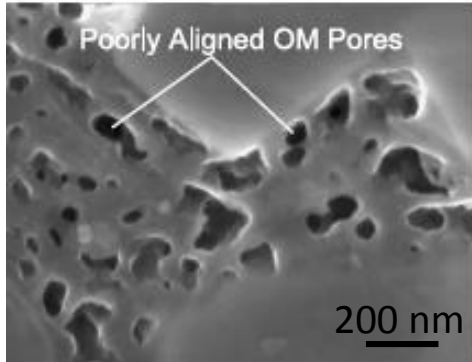
US Energy Information Administration (EIA) - 2013

Shale porosity

Pores are at nanoscale

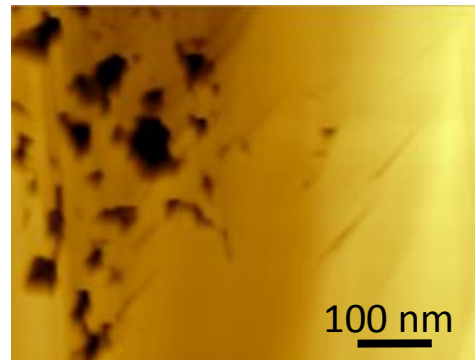
Direct methods

SEM



(Loucks et al.,
AAPG, 2012)

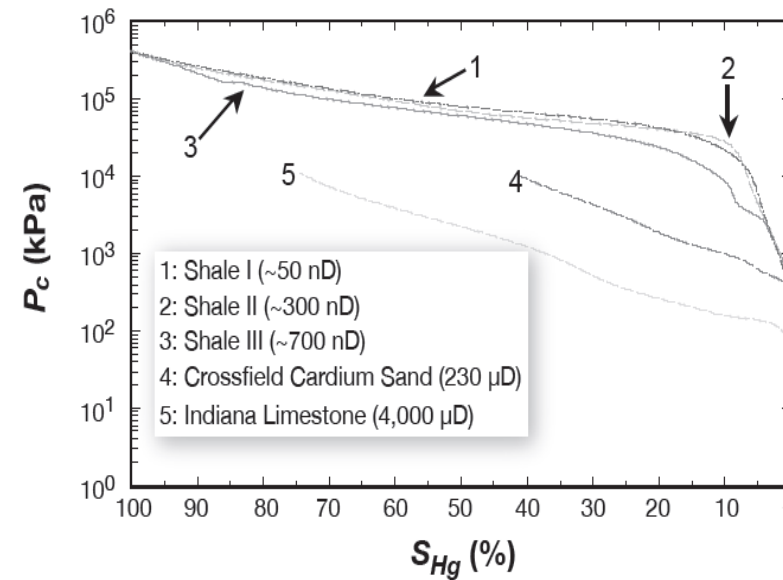
AFM



(Javadpour et al.,
JCPT, 2012)

Indirect methods

MICP tests

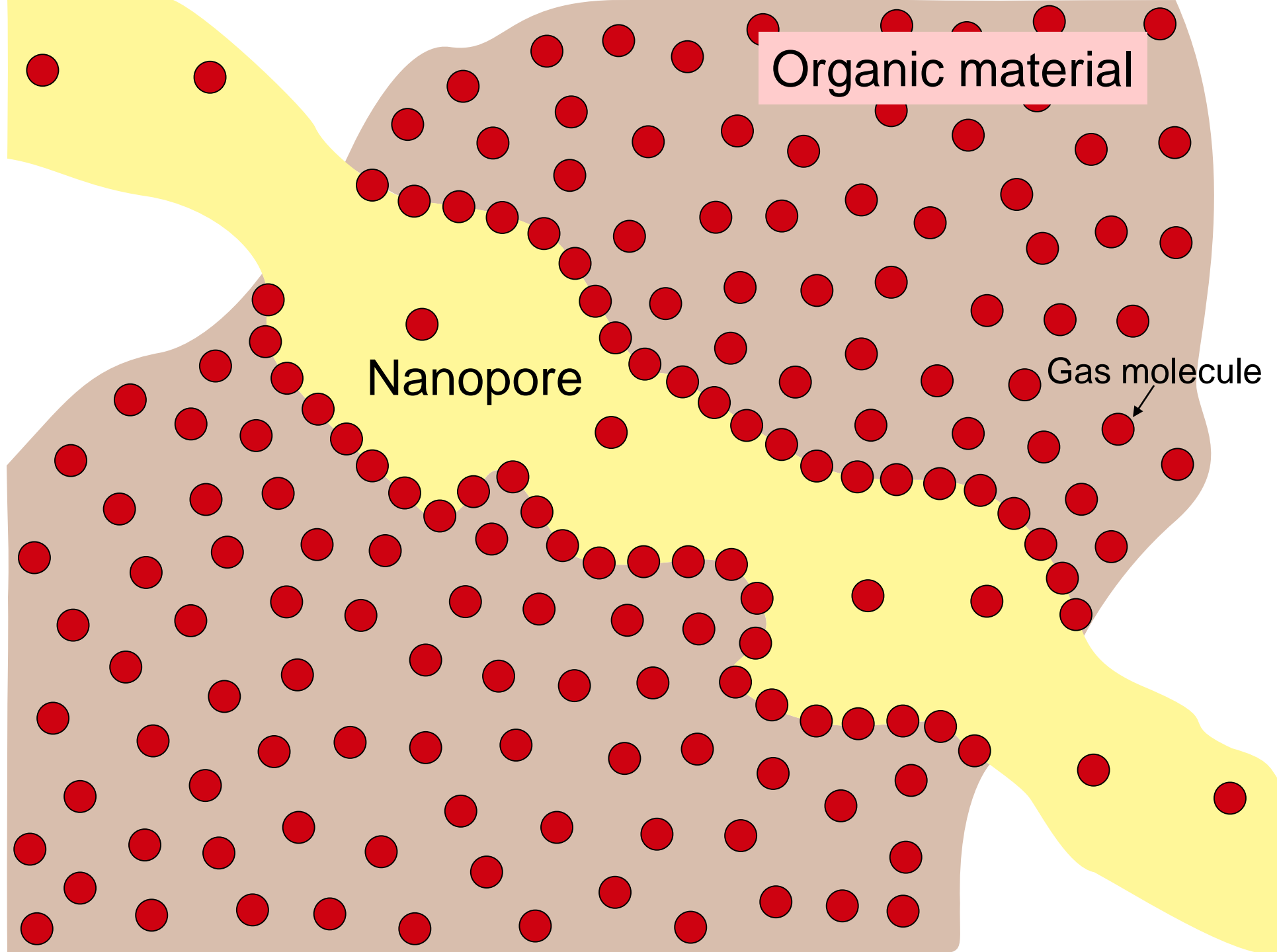


(Javadpour et al.,
JCPT, 2007)

Nitrogen tests

Pore dia. (nm)	Fraction (%)
5.0	11.5
7.5	16.0
12.5	10.5
17.5	12.0
22.5	7.0
27.5	8.0
32.5	4.0
170.0	31.0

(Courtesy Dr. Zhang)



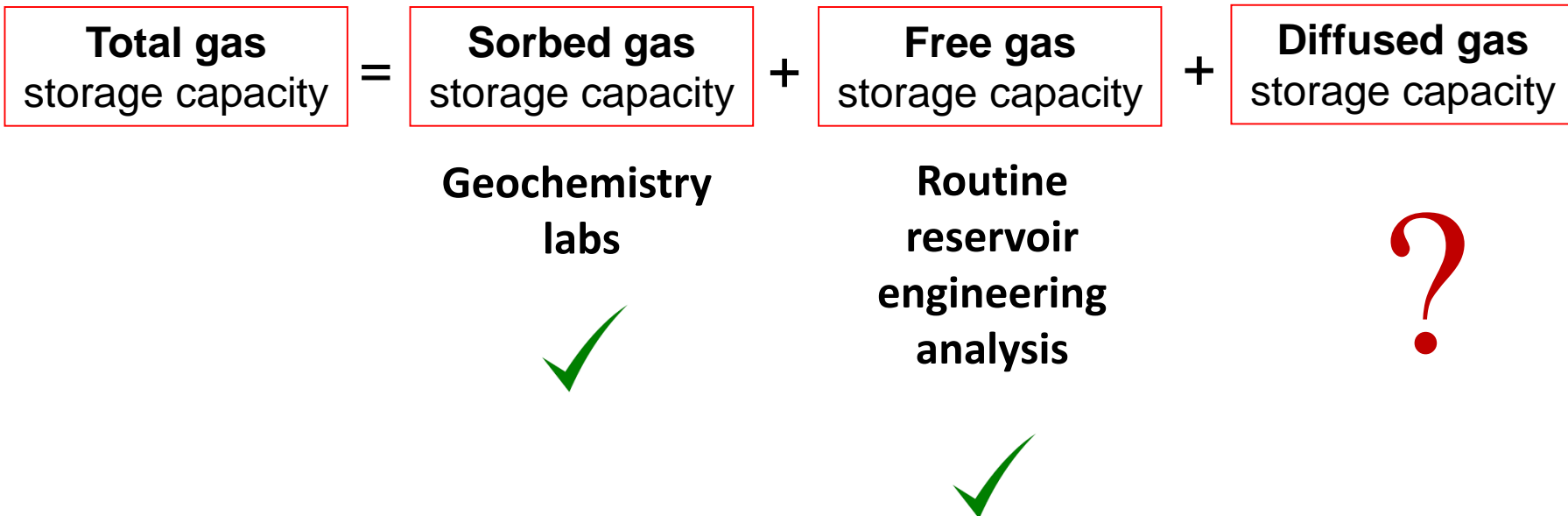
Organic material

Nanopore

Gas molecule

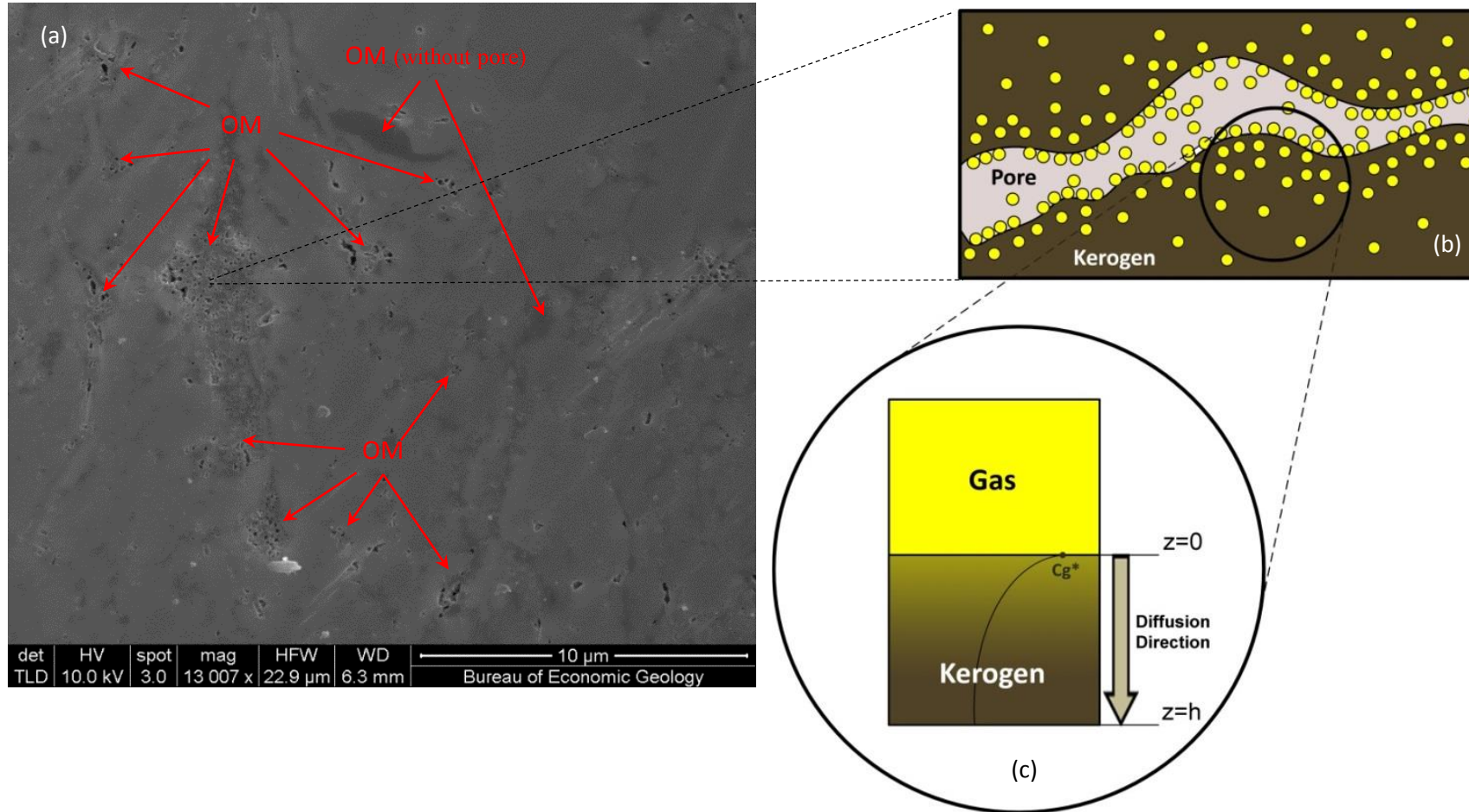
Total gas stored in shale gas strata

$$G_{st} = G_s + G_{cf} + G_{sd}$$

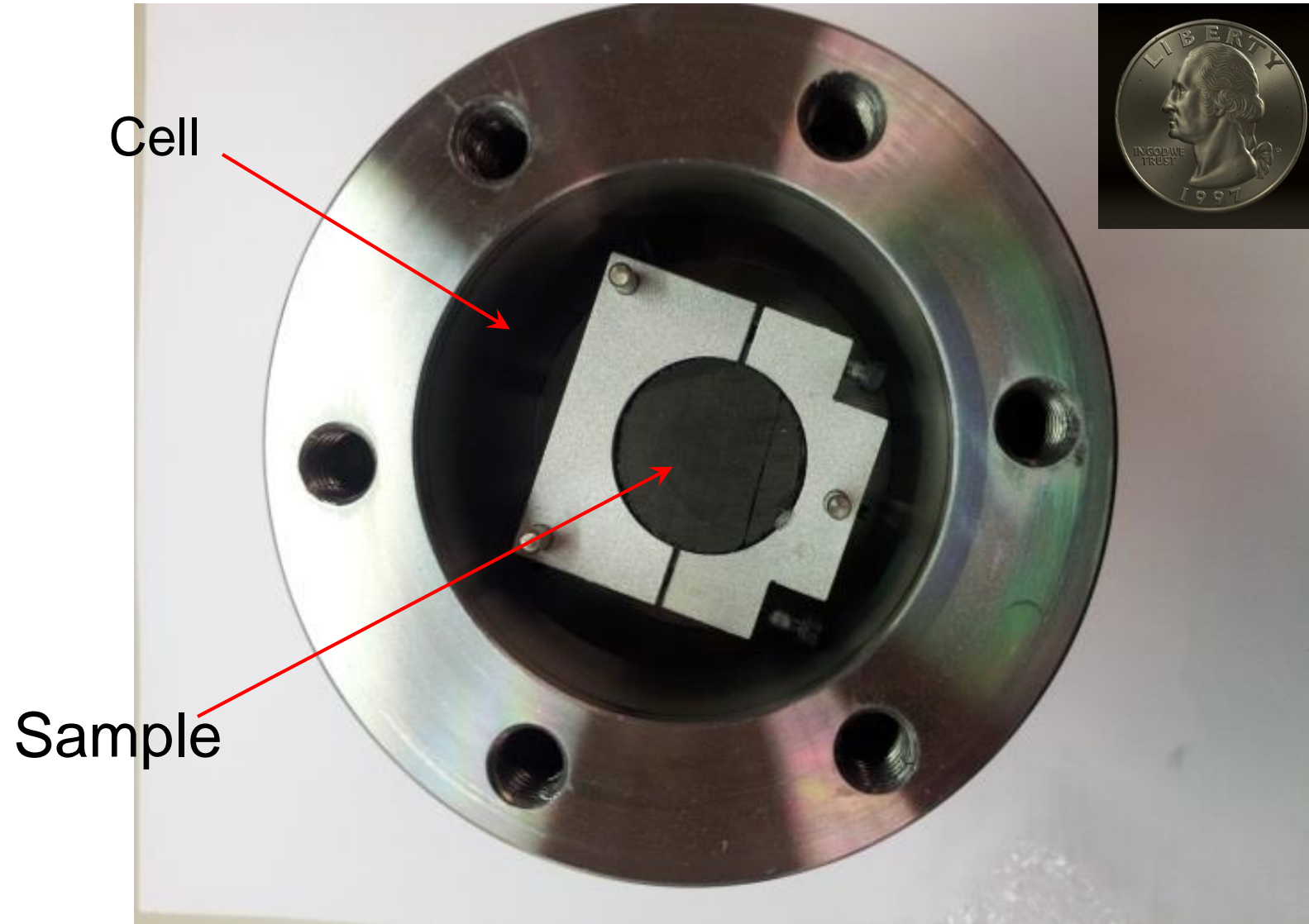


Diffusion in kerogenic material

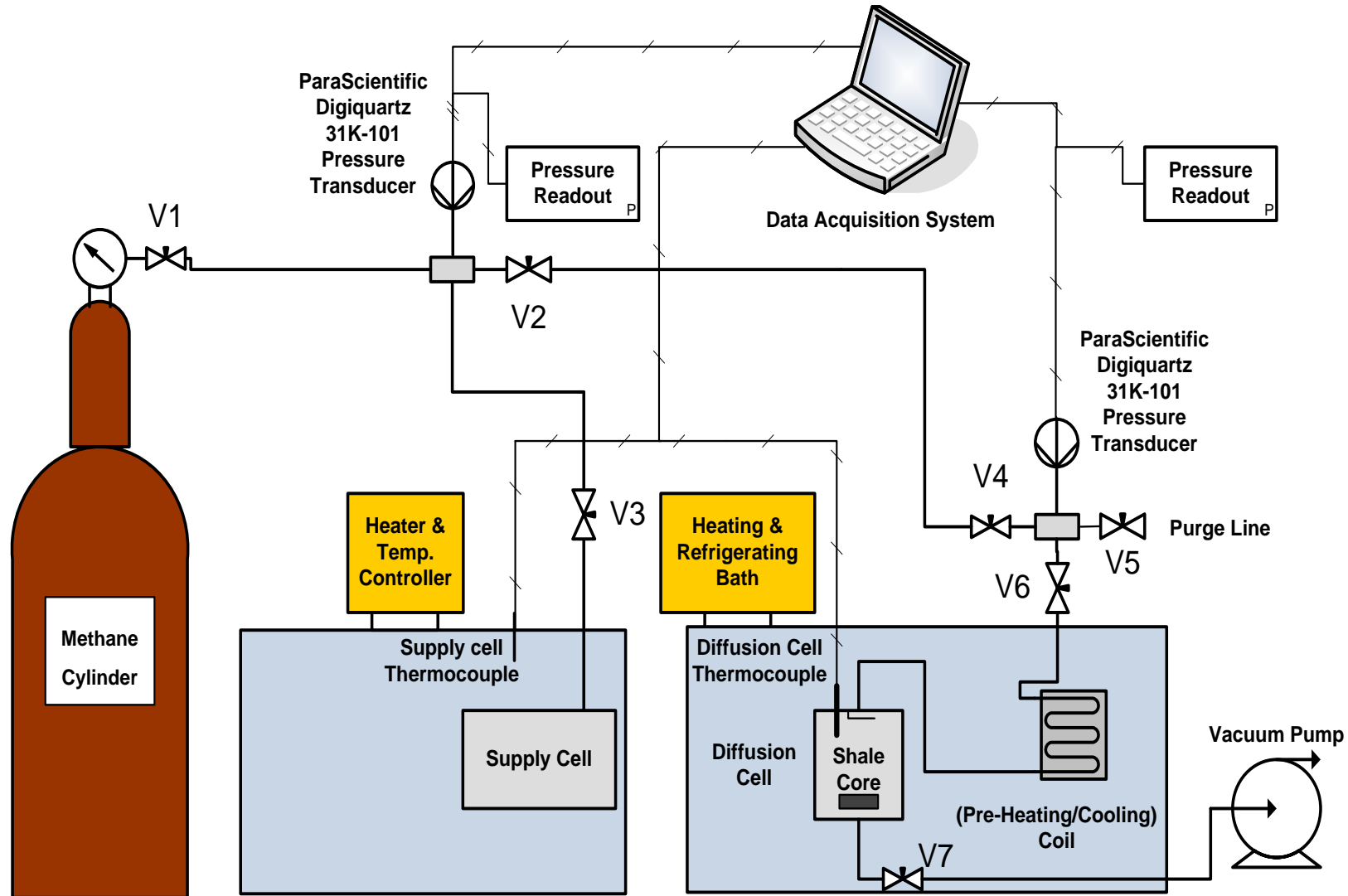
Diffused gas in bulk kerogen



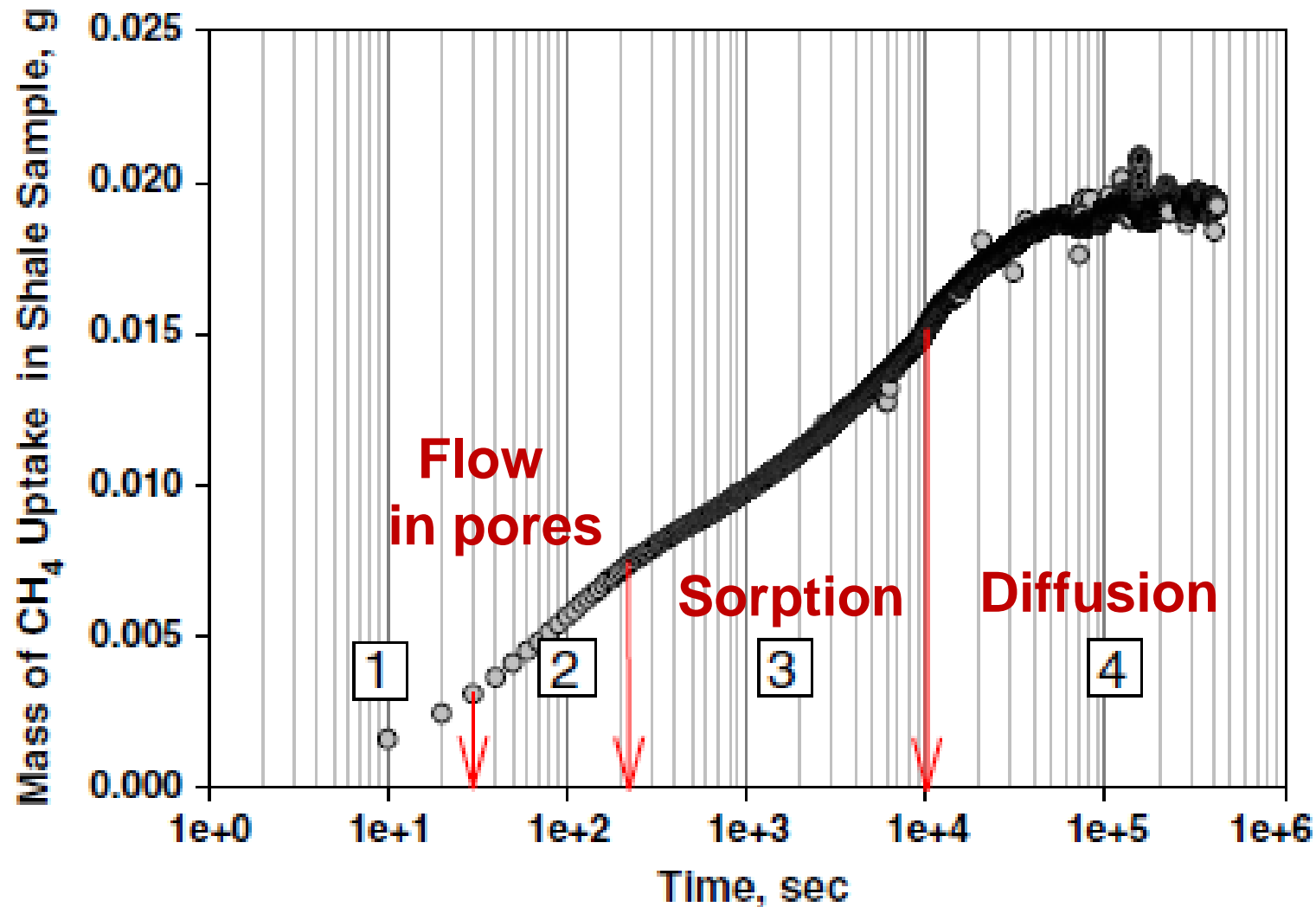
Pressure cell and sample



High precision pressure cell



Conversion of pressure data to mass

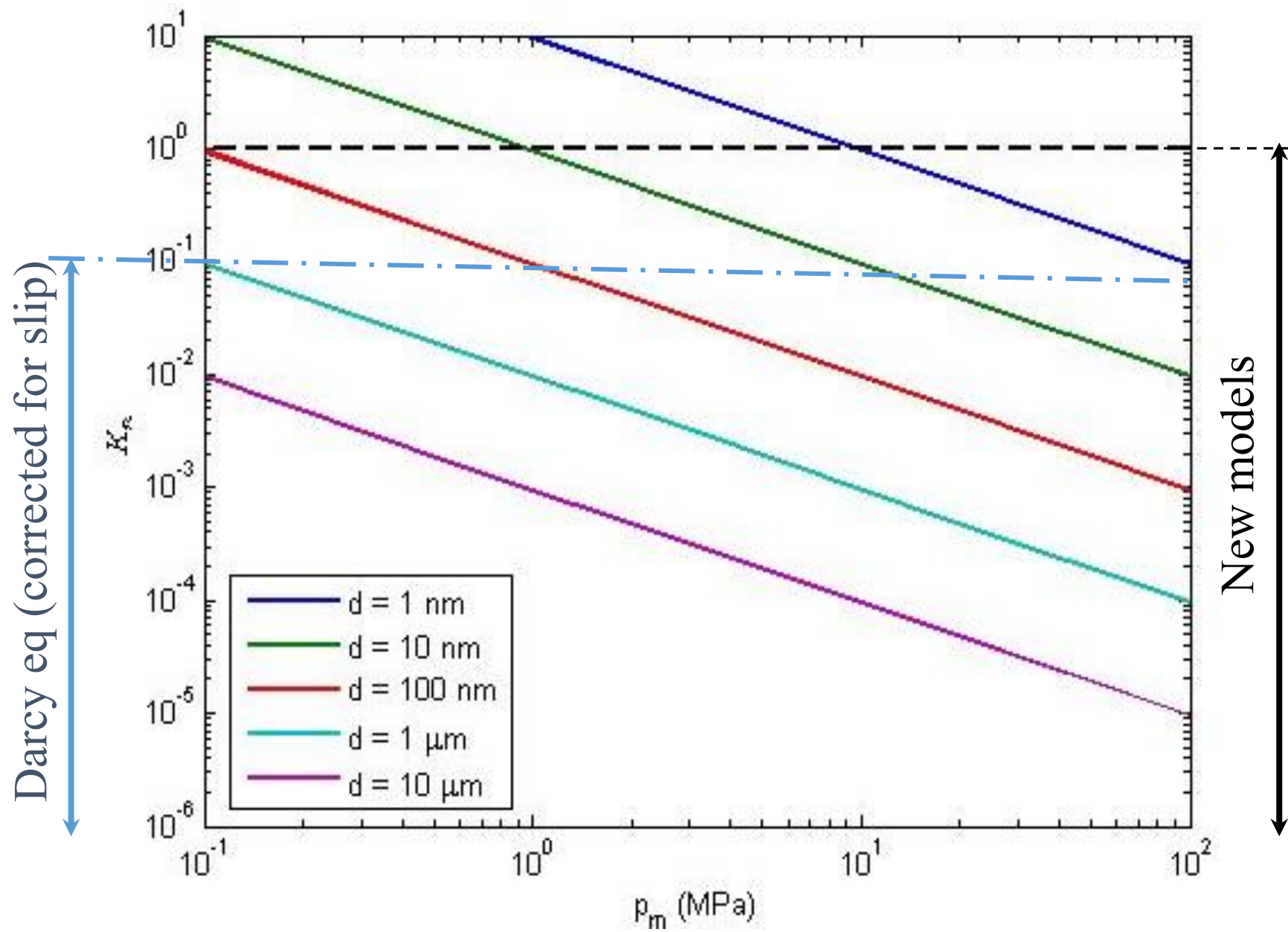


Etminan et al., International Journal of Coal Geology (2014)

Gas flow in nanopores

Different flow regimes as a function of Knudsen number.

	Knudsen number (K_n)		Flow regime	
	Lower bound	Upper bound		
Validity of the LSP model	0	10^{-3}	Continuum/Darcy flow (No-slip flow)	Navier-Stokes Equation
	10^{-3}	10^{-2}	Slip flow	
	10^{-2}	10^{-1}		
	10^{-1}	10^0	Transition flow	
	10^0	10^1		
	10^1	∞	Free-molecule flow	



Apparent permeability of nanopores

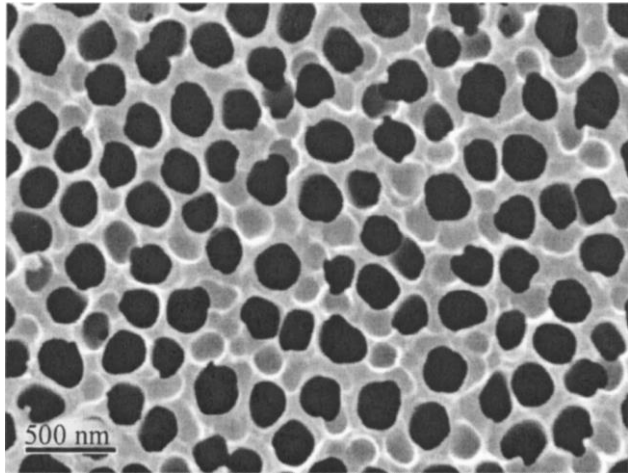
$$k_{app} = \frac{2r\mu M}{3 \times 10^3 RT \rho_{avg}} \left(\frac{8RT}{\pi M} \right)^{0.5} + F \frac{r^2}{8}$$

$$F = 1 + \left(\frac{8\pi RT}{M} \right)^{0.5} \frac{\mu}{p_{avg} r} \left(\frac{2}{\alpha} - 1 \right)$$

Compare to Darcy eq.

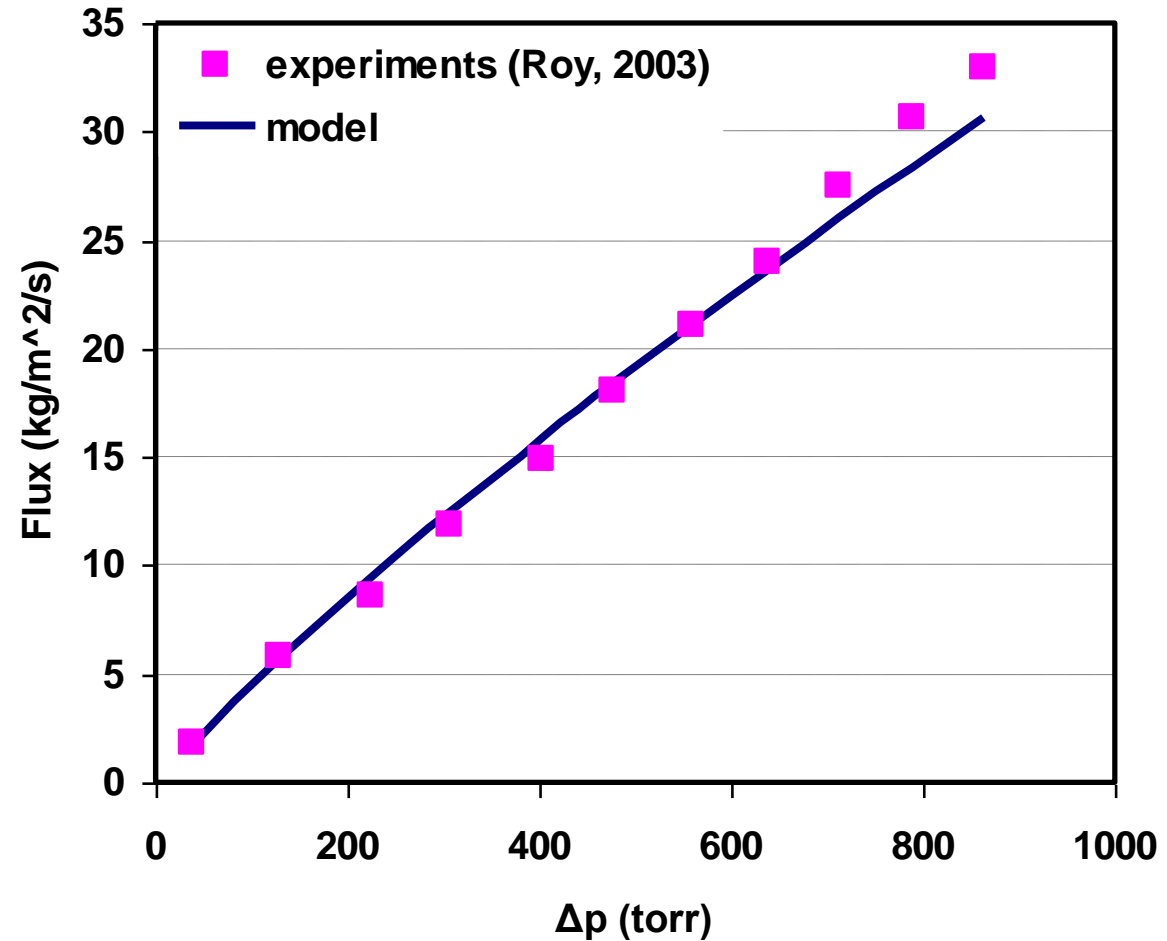
$$k_{Darcy} = \frac{r^2}{8}$$

Validation with experimental data

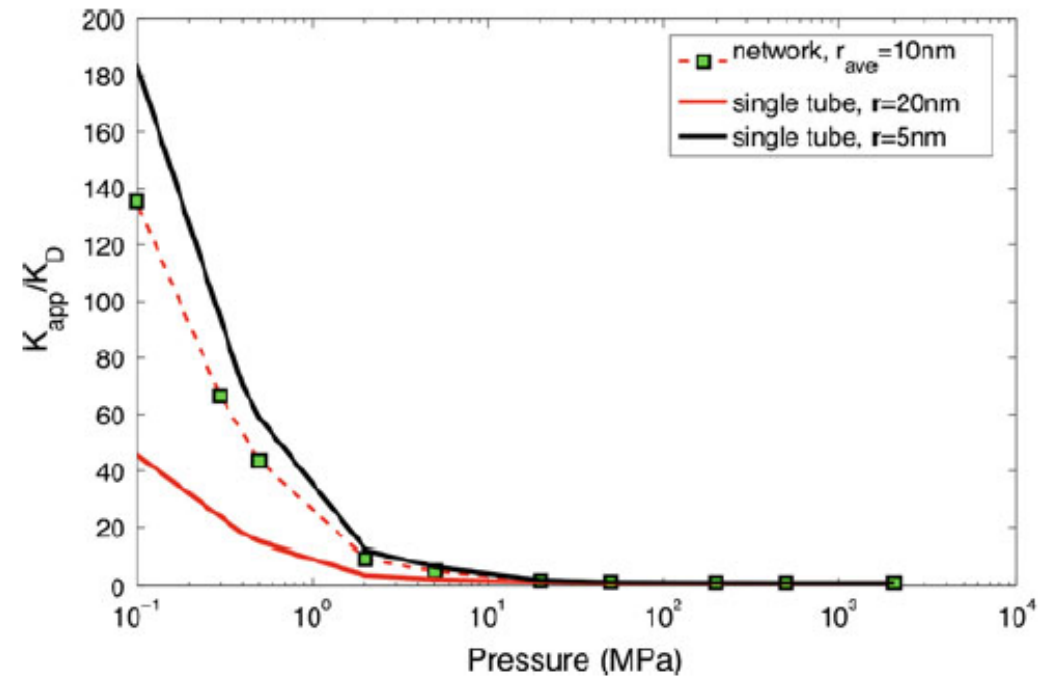
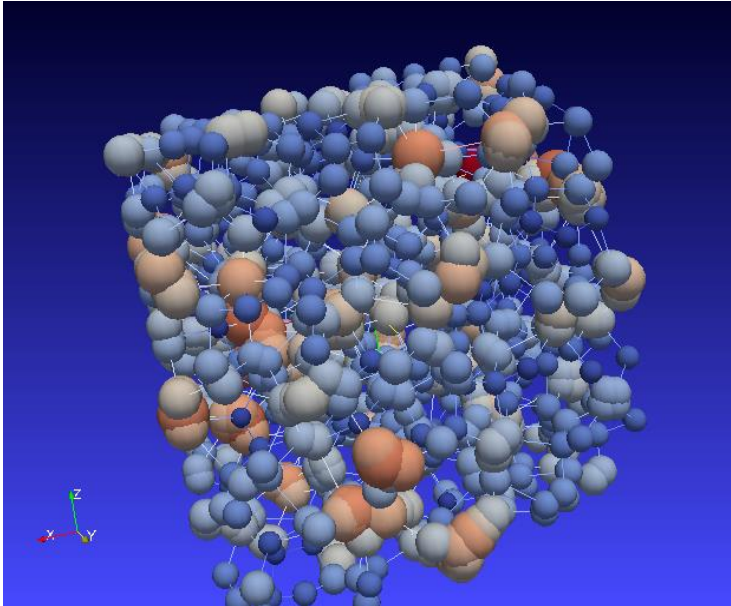


Artificial nanopores

NASA Ames Research Center



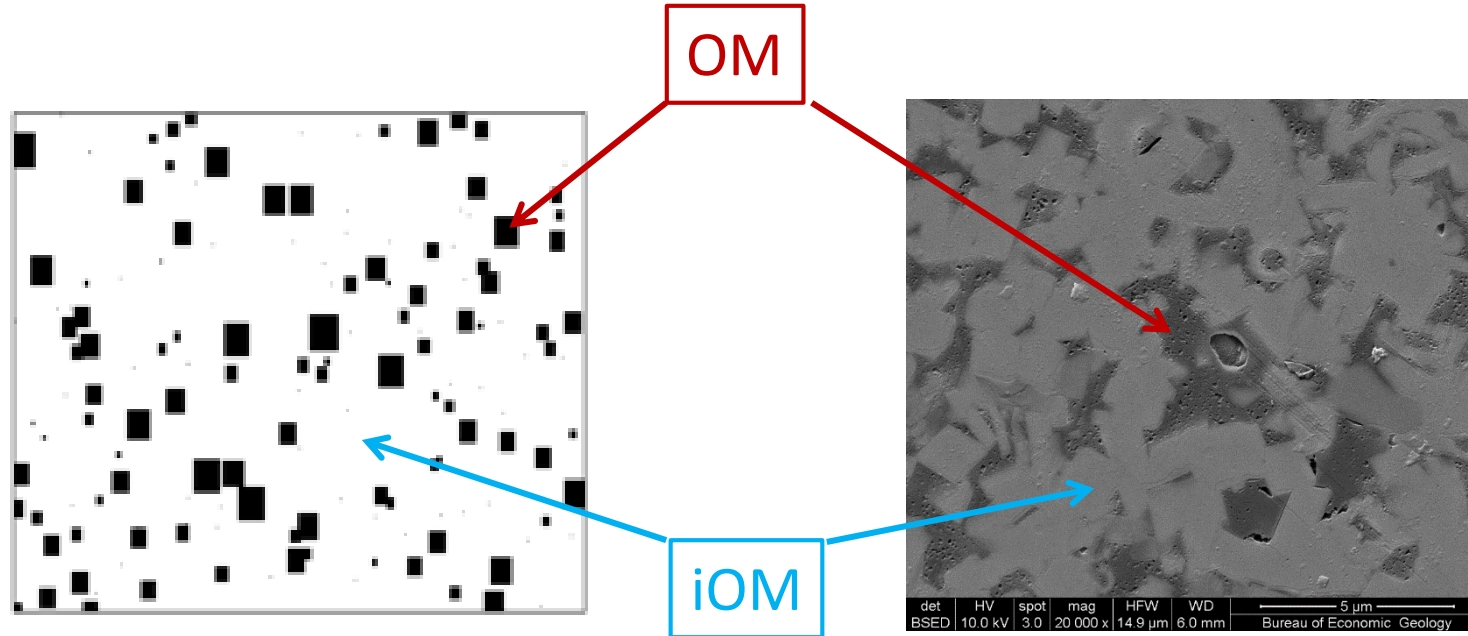
Pore network model



Mehmani et al., Transport in Porous Media (2013)

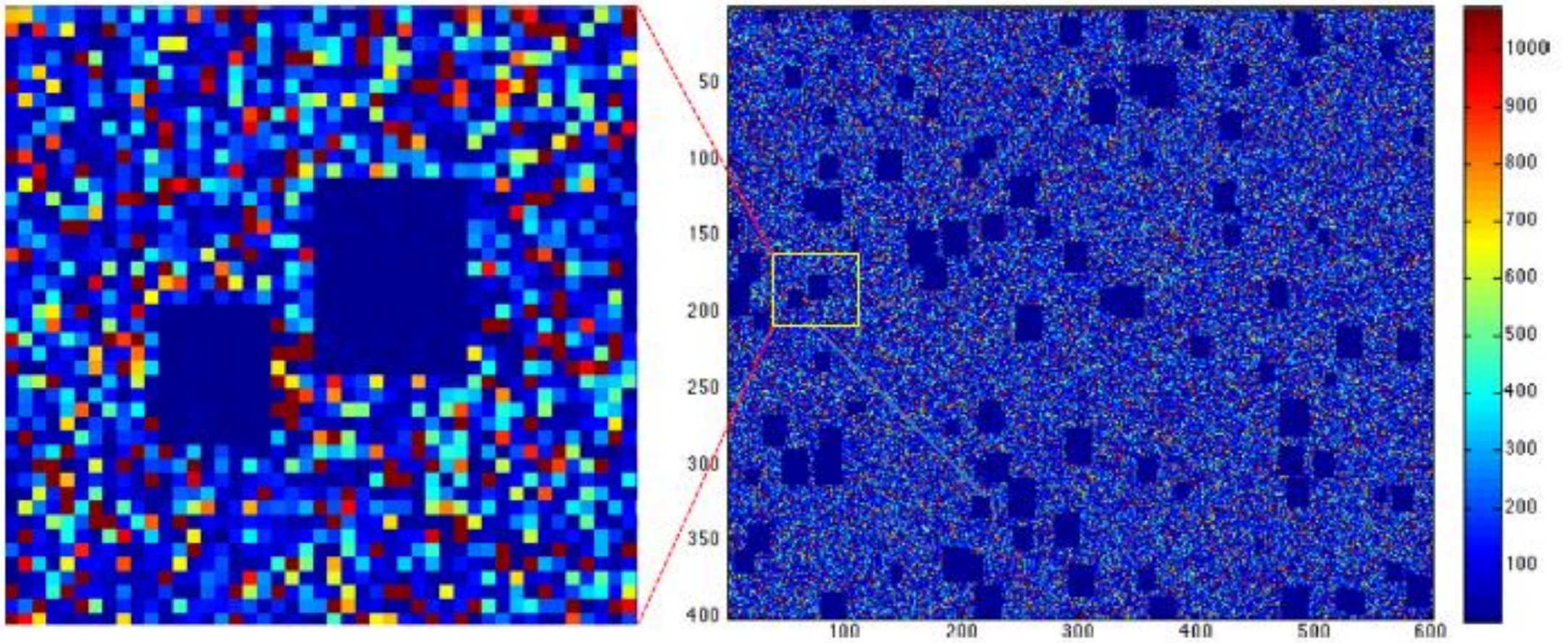
Stochastic permeability model

SEM to permeability



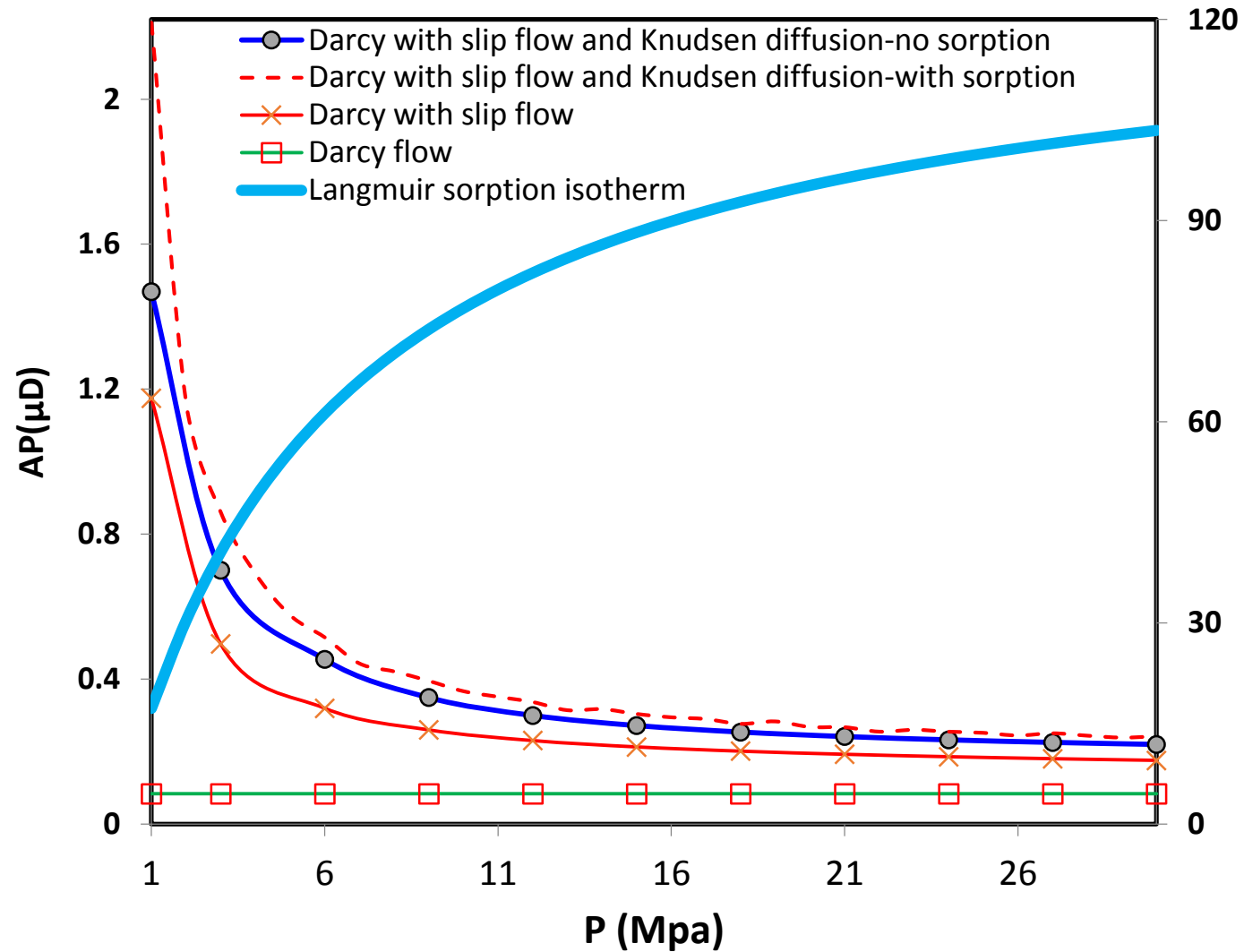
- TOC
- OM patch SD from SEM images
- Pore SD in OM & iOM from N_2 & MICP

Stochastic model

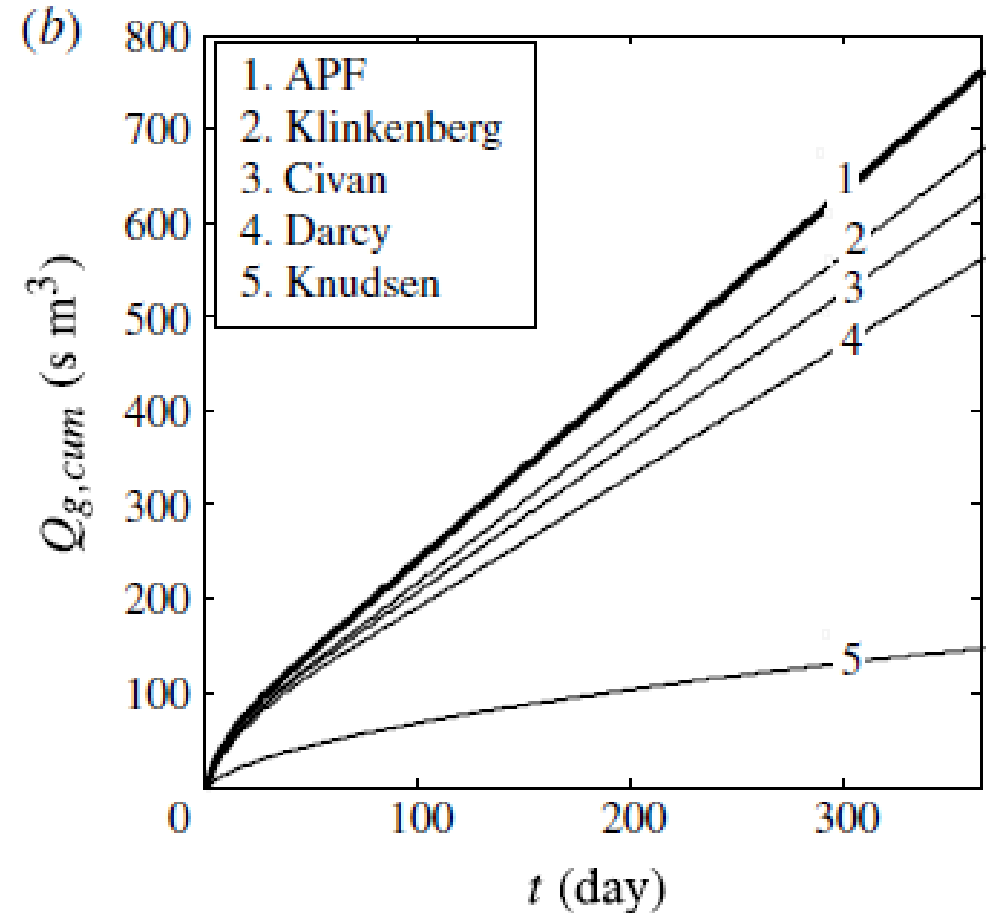
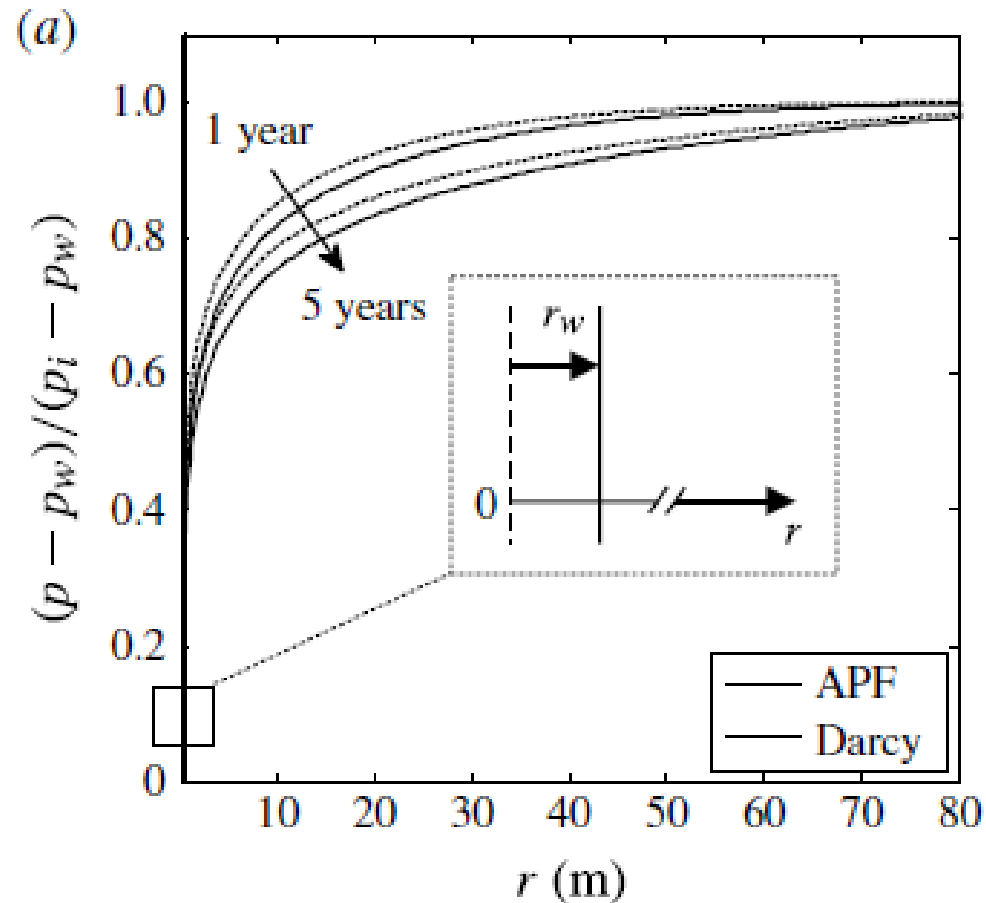


Naraghi & Javadpour, International Journal of Coal Geology (2015)

Effect of sorption



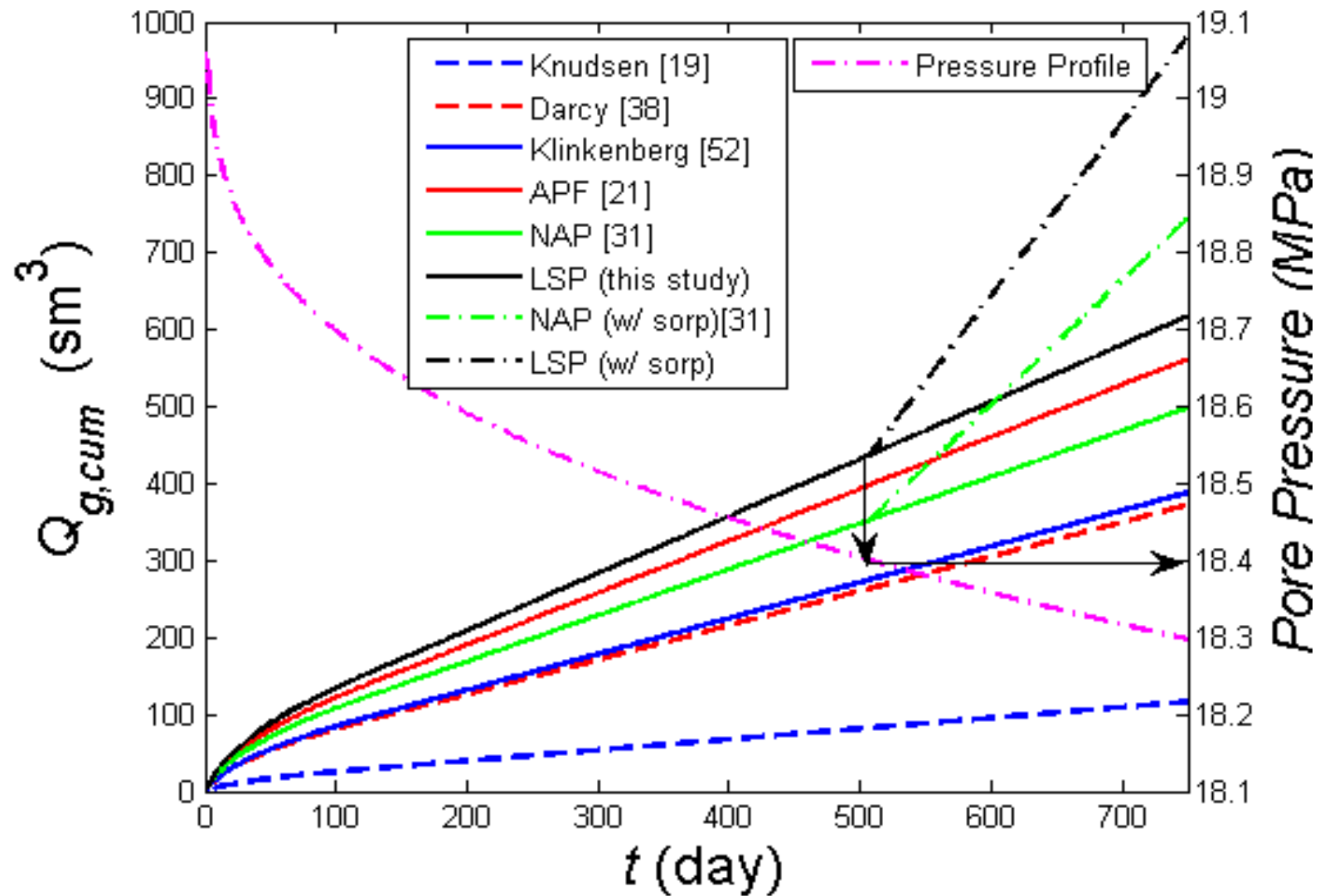
Reservoir model



Model	Description	Pros	Cons
Javadpour (2009)	Model developed using slip flow assumption, represented by Maxwell theory. Accounts for Knudsen diffusion.	Simple.	Limited to straight tubes. Ideal gas. Ignores desorption.
Civan (2010)	Model developed using slip flow assumption, represented by simplified second-order slip model. Contains several empirical parameters	Higher-order slip flow.	Several empirical parameters.
Darabi et al. (2012)	Model developed using slip flow assumption, represented by Maxwell theory. Accounts for surface roughness and Knudsen diffusion in a porous medium.	Includes tortuosity and pore surface roughness.	Needs TMAC values. Ideal gas. Ignores desorption.
Akkutlu & Fathi (2012)	Model includes dual-porosity continua of matrix/fracture system, where matrix is composed of both organic and inorganic pores. Accounts for surface diffusion and sorption.	Dual-porosity system.	Complex numerical model.
Shabro et al. (2012)	A finite-difference based numerical model and geometrical parameters are used to reconstruct porous structure of shale, which is then used for pore-scale characterization. Permeability equation is borrowed from Javadpour (2009).	Spatial characterization and geometry of porous media included.	Complex numerical model. Ideal gas. Ignores desorption. Needs TMAC values.
Sakhaee-Pour & Bryant (2012)	Model developed using slip flow assumption, represented by Maxwell theory. Accounts for Knudsen diffusion.	Spatial characterization and geometry of porous media included.	Needs TMAC values. Ideal gas.
Mehmani et al. (2013)	Model developed by employing flow equation from Javadpour (2009) in pore network interconnected on nano and micro length scales.	Spatial characterization and geometry of porous media included.	Complex numerical model. Ideal gas. Ignores desorption. Needs TMAC values.
Singh et al. (2014)	Model developed using Navier-Stokes equation and kinetic theory (no slip flow assumption). Accounts for Knudsen diffusion, porous medium and sorption.	Simple. No empirical coefficient.	Ignores slip flow.
Rezaveisi et al. (2014)	Numerical model developed to study components of produced gas with time from nanometer sized pores. Relevant physics includes advection, slip flow and Knudsen diffusion.	Distinguishes different gas types.	Needs TMAC values.
Kelly et al. (2015)	Porous structure of shale is reconstructed using FIB-SEM image stacks and numerical study using LBM is performed to study petrophysical properties of shale. Permeability estimation is done using pressure driven flow.	Spatial characterization and geometry of porous media included.	Complex numerical model. Ignores slip, diffusion and desorption.
Chen et al. (2015)	Porous structure of shale is reconstructed using Markov Chain Monte Carlo (MCMC) on SEM images and its pore-scale characterization is performed. Apparent permeability includes flow from advection, Knudsen diffusion and slip. LBM is used to simulate fluid flow.	Spatial characterization and geometry of porous media included.	Complex numerical model. Ignores desorption. Several empirical parameters.
Naraghi & Javadpour (2015)	Model developed by stochastically characterizing organic and inorganic pores. Accounts for slip flow, Knudsen diffusion, surface roughness and desorption.	Distinguishes different pore systems in organic and inorganic matter. Real gases.	Needs additional information from SEM images. Needs TMAC values.
Singh & Javadpour (2015)	Model developed using the Langmuir slip condition and it does not carry several shortcomings associated with the use of Maxwell slip. Reliably predict apparent permeability in shale.	Simple and analytic. Gets slip coefficient from sorption data. Real gas.	Ignores local heterogeneity.

Model Name	Equation	Empirical Parameters	Description of Parameters
Knudsen	$\frac{2\phi r\mu M}{3 \times 10^3 \tau RT \rho^2} \left(\frac{8RT}{\pi M} \right)^{0.5}$	None	None
Darcy	$\frac{\phi r^2}{8\tau}$	None	None
Klinkenberg	$\frac{\phi r^2}{8\tau} \left(1 + \frac{b}{p} \right)$	b	Accounts for gas slip
APF	$\frac{\phi \mu M (\delta')^{D_f - 2} D_k}{\tau RT \rho} + \frac{\phi r^2}{8\tau} \left(1 + \frac{b}{p} \right)$	δ', D_f, b	Account for normalized molecule to pore size, pore roughness and slip, respectively
NAP	$\frac{4\phi \mu r}{\tau \pi} \left(\frac{\pi r z}{32\mu} + \frac{1}{3pM} \sqrt{2\pi MRT} \right)$	None	None
LSP (Singh & Javadpour, 2015)	$-\frac{\phi h^2}{4\tau} \left(\frac{1}{\left(-\frac{dP}{dX} \right)_{X=1} \left(2 + \frac{3}{\sqrt{\bar{\beta}}} \right)} \right) \frac{dP}{dX} \left(\frac{2}{3} + \frac{1}{\sqrt{\bar{\beta} P}} \right)$	$\bar{\beta}$	Dimensionless form of β which accounts for higher-order Langmuir slip

More reservoir models



Lost gas estimation from canister tests

Gas content from canister tests

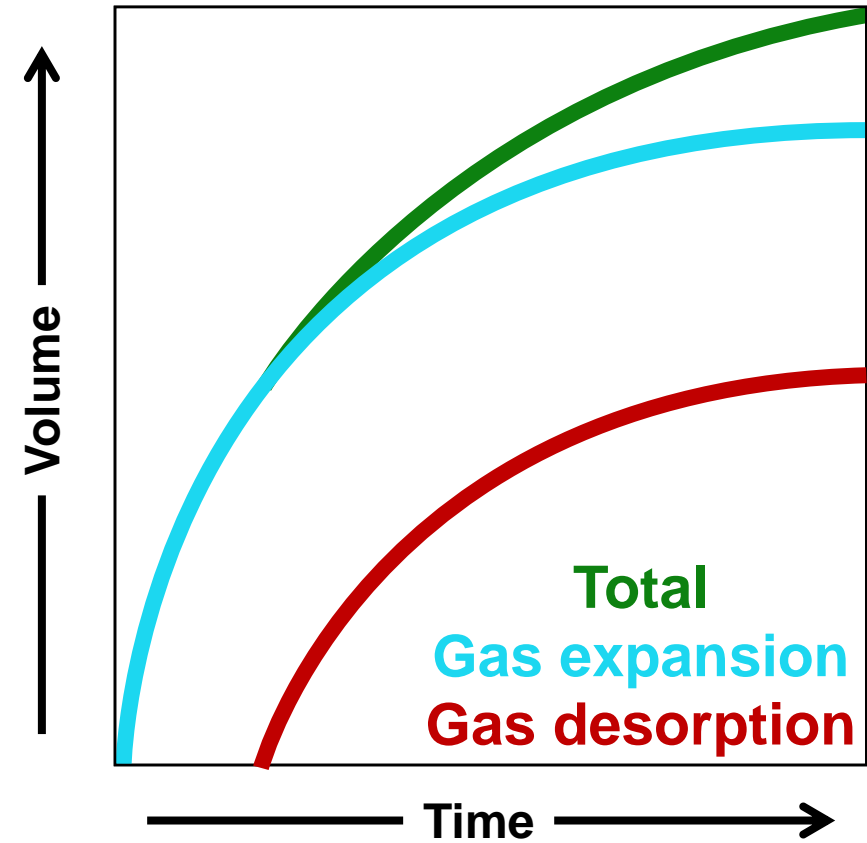
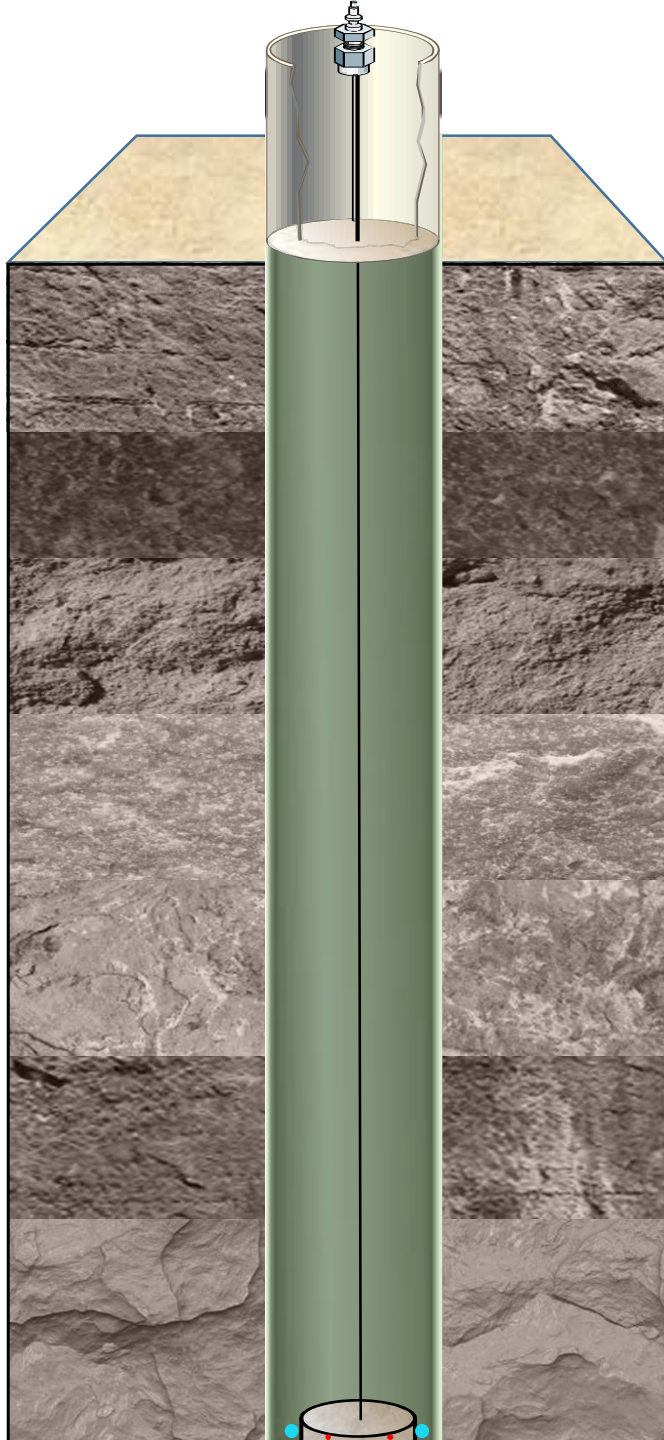
- Is the volume of gas released from a reservoir shale sample
- It is used to calculate gas-in-place volume for a reservoir
- Total gas content of a shale sample consists of three components:

lost gas (Q1)

measured gas (Q2)

residual gas (Q3)

Core retrieval



Canister Gas

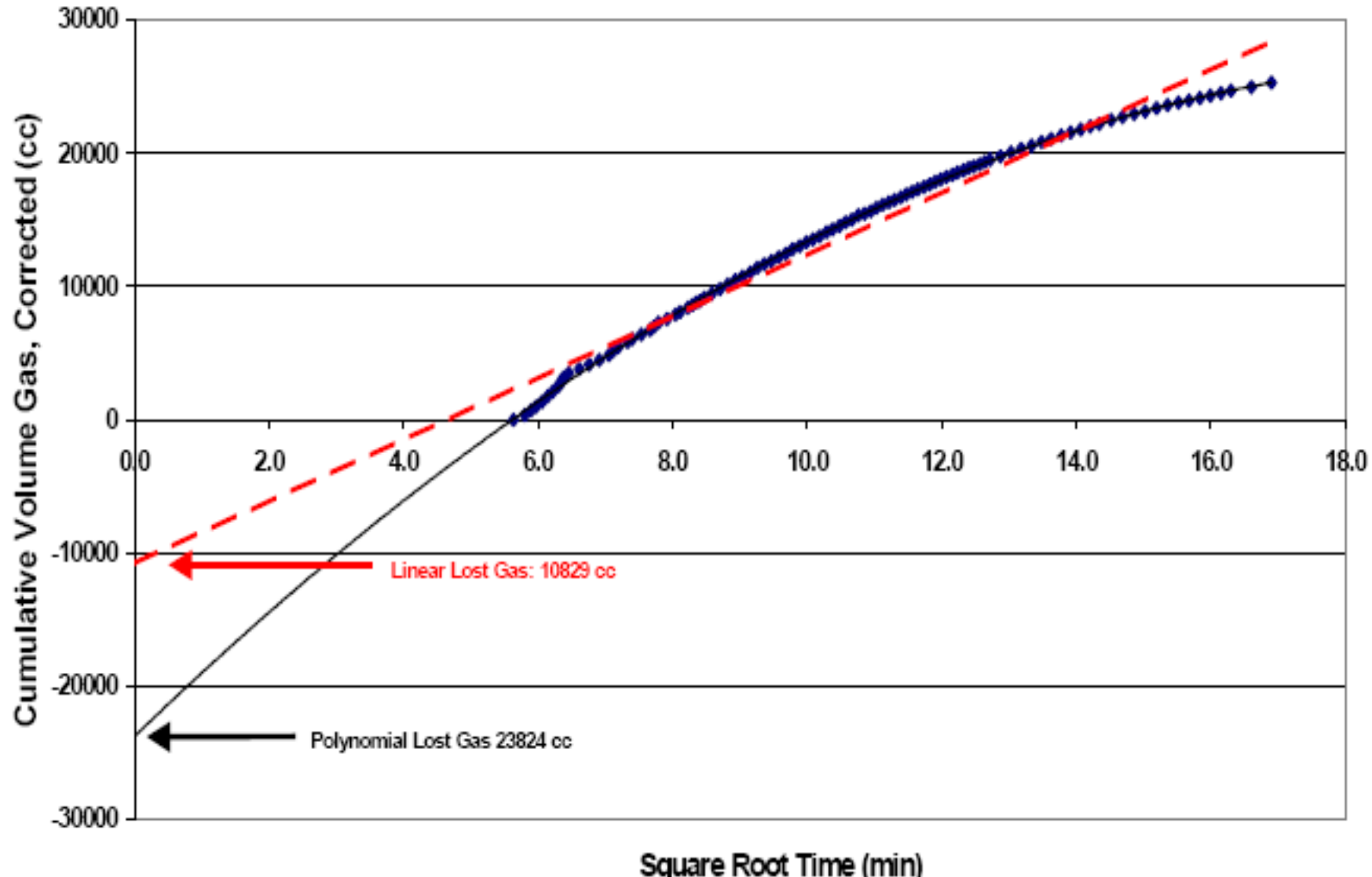
- Reservoir temperature
- Lost gas + measured gas + crushed gas
- Adsorbed gas in CBM
- Free + adsorbed gas in shale

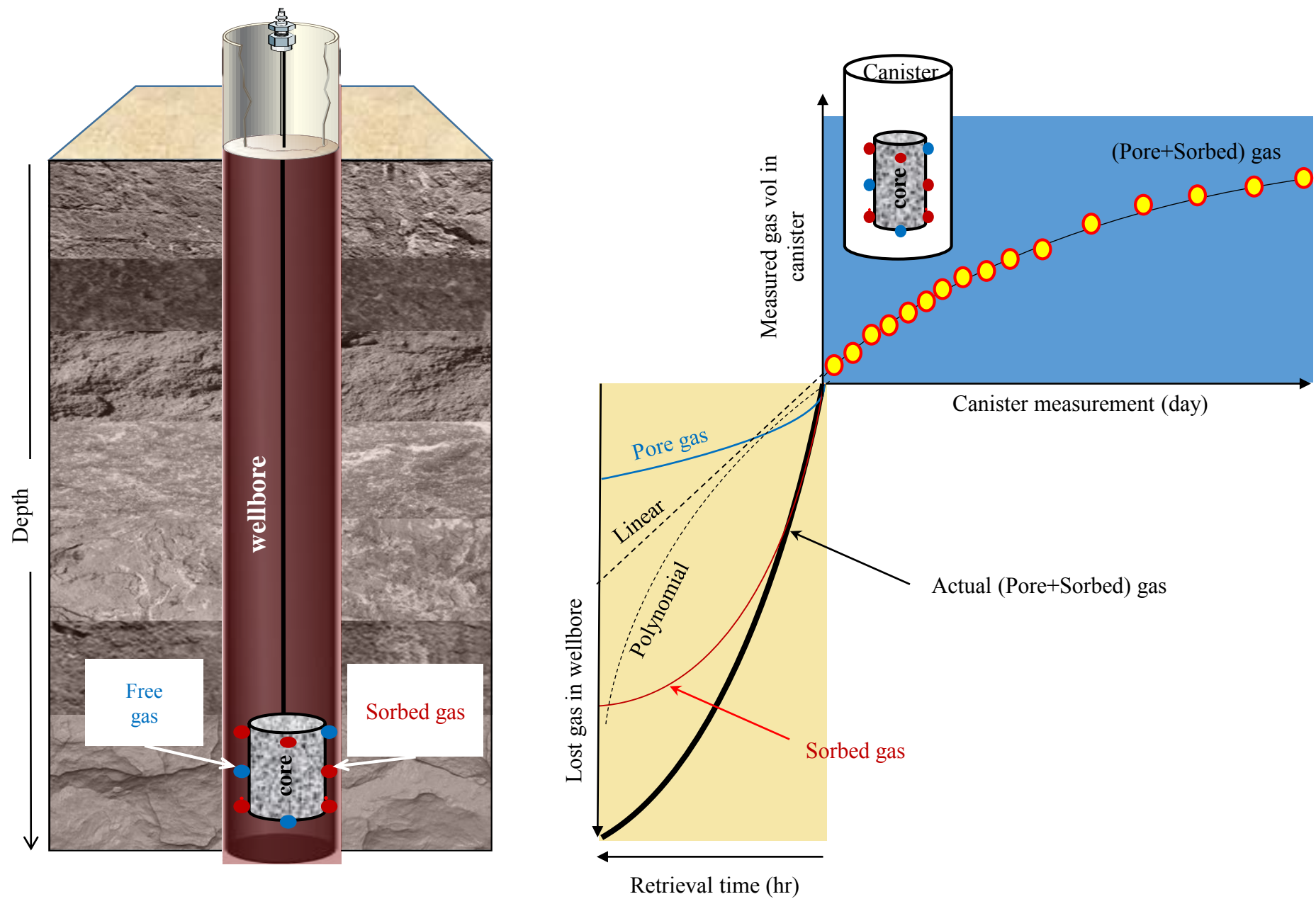


Waechter et al. World Oil, 2004

Lost gas estimation

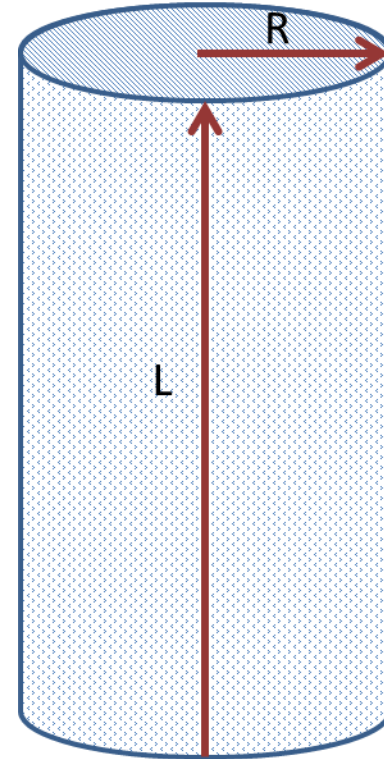
Linear fit vs polynomial





PDE, BC and IC

- $\phi c \frac{\partial P}{\partial t} = \frac{1}{r} \frac{\partial(r v_r)}{\partial r} + \frac{\partial(v_z)}{\partial z} + R$
- B.C. and I.C.
 - $P(r = R, z, t > 0) = f(t)$
 - $P(r, z = L, t > 0) = f(t)$
 - $P(r, z = 0, t > 0) = f(t)$
 - $P(r, z, 0) = P_i$



Solution in real domain

- After few steps:

$$\begin{aligned} \text{➤ } P_D(r_D, z_D, t_D) = & e^{-\beta t_D} + \\ & 2 \sum_{m=1}^{inf} \left\{ \left[2 \sum_{n=1}^{inf} \left\{ \left[e^{\frac{-t_D(\omega_m^2 v^2 + \lambda_n^2)}{(\alpha+1)}} - e^{-\beta t_D} \right] \frac{\beta(\alpha+1)(1-\cos(\omega_m))F(\lambda_n)}{(\beta(\alpha+1) - \omega_m^2 v^2 - \lambda_n^2)\omega_m} \right\} \frac{J_0(\lambda_n r_D)}{|J_1(\lambda_n)|^2} \right] \sin(\omega_m z_D) \right\} \end{aligned}$$

$$\text{➤ } \omega_m = m\pi \quad m = 1, 2, \dots$$

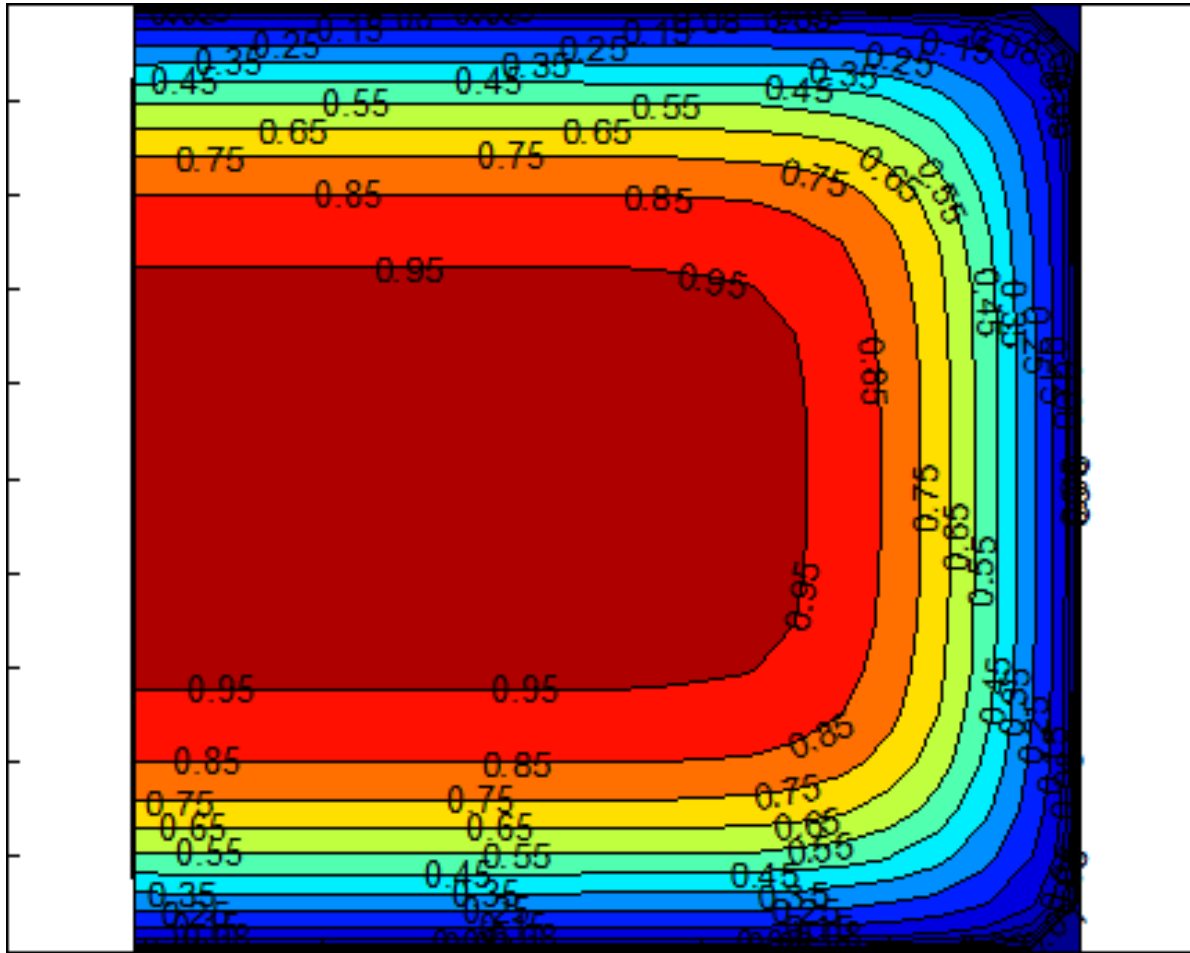
$$\text{➤ } \lambda_n = J_0(0, n) \quad n = 1, 2, 3, \dots$$

- Average pressure:

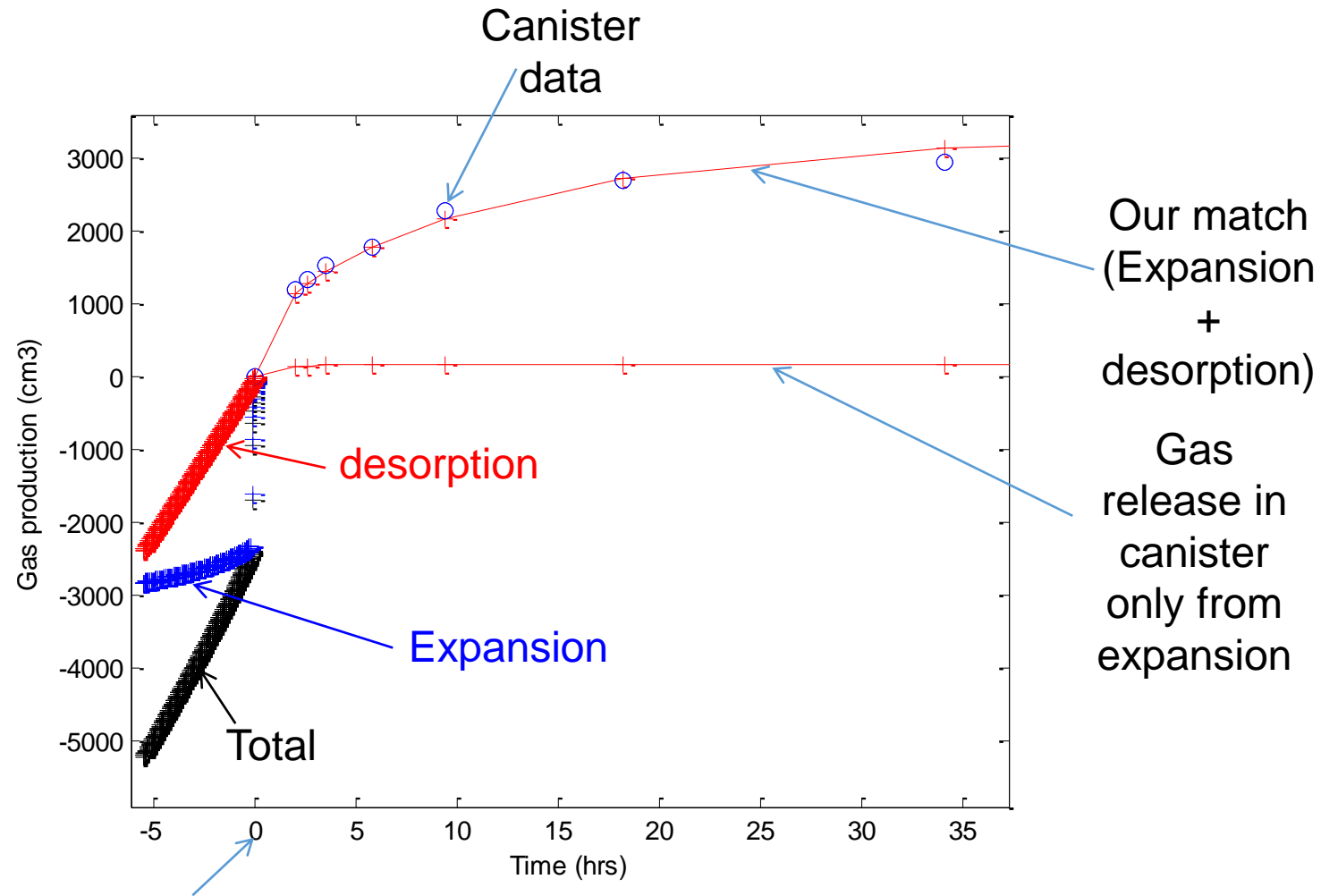
$$\text{➤ } \overline{P_D}(t_D) = \frac{1}{V} \int_0^1 \int_0^1 P_D(r_D, z_D, t_D) dz_D dr_D$$

$$\text{➤ } \overline{P_D}(t_D) = \frac{1}{\pi} \left[e^{-\beta t_D} + 4 \sum_{m=1}^{inf} \sum_{n=1}^{inf} \left[e^{\frac{-t_D(\omega_m^2 v^2 + \lambda_n^2)}{(\alpha+1)}} - e^{-\beta t_D} \right] \frac{\beta(\alpha+1)(1-\cos(\omega_m))^2}{(\beta(\alpha+1) - \omega_m^2 v^2 - \lambda_n^2)\lambda_n^2 \omega_m^2} \right]$$

Pressure profile



Rigorous estimation of lost gas

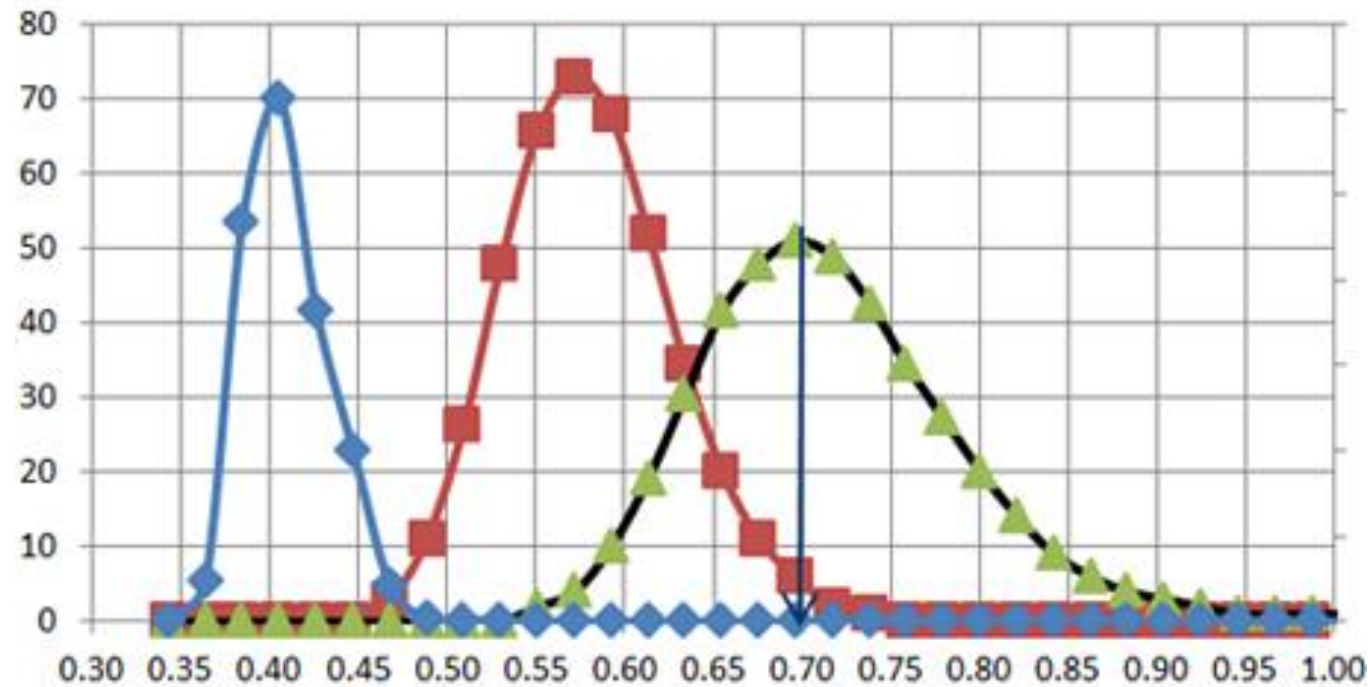
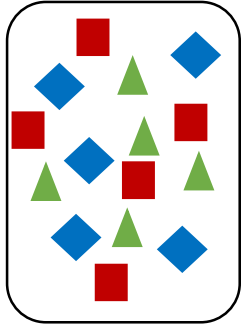


Time zero represents the time core is placed in canister

Hosseini et al., SPE Journal, 2015

**In-situ gas
chromatographic
separation (CS) in shale
reservoirs**

Chromatographic separation (CS)



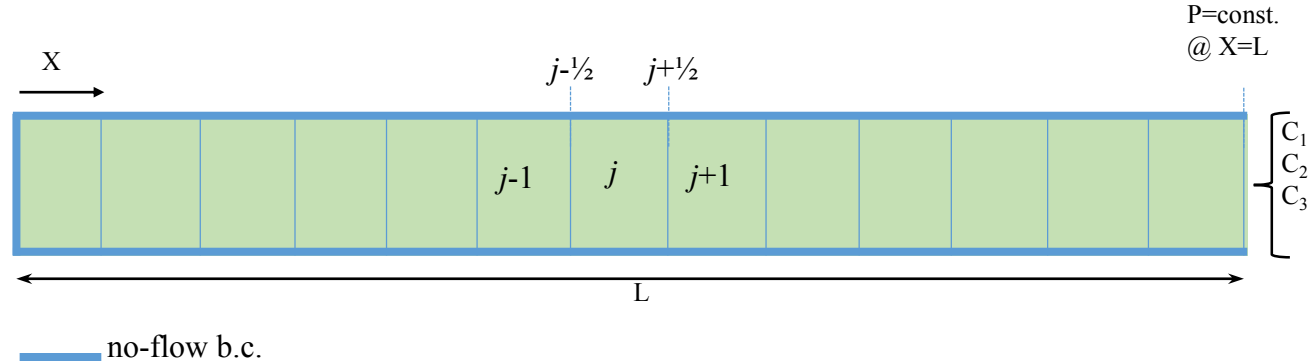
Field observation (Freeman, Moridis, Michael, Blasingame, 2012)

Temporal variation of gas composition in produced gas

Is the observed variation related to an in-situ separation process?

If yes, how we control the composition variation?

Governing equations



$$\frac{\partial(\phi \rho y_i)}{\partial t} = -\frac{\partial}{\partial x} \left[-y_i \rho \frac{k_D}{\mu} \left(1 + \frac{b_i}{P} \right) \frac{\partial P}{\partial x} - \frac{D_{k,eff,i}}{RT} \frac{\partial}{\partial x} \left(\frac{P y_i}{Z} \right) \right] + r_i$$

$$P_{(x, t = 0)} = P_i$$

$$y_{i(x, t = 0)} = y_{i0} \quad \text{for } i = 1, 2, \dots, N_c - 1$$

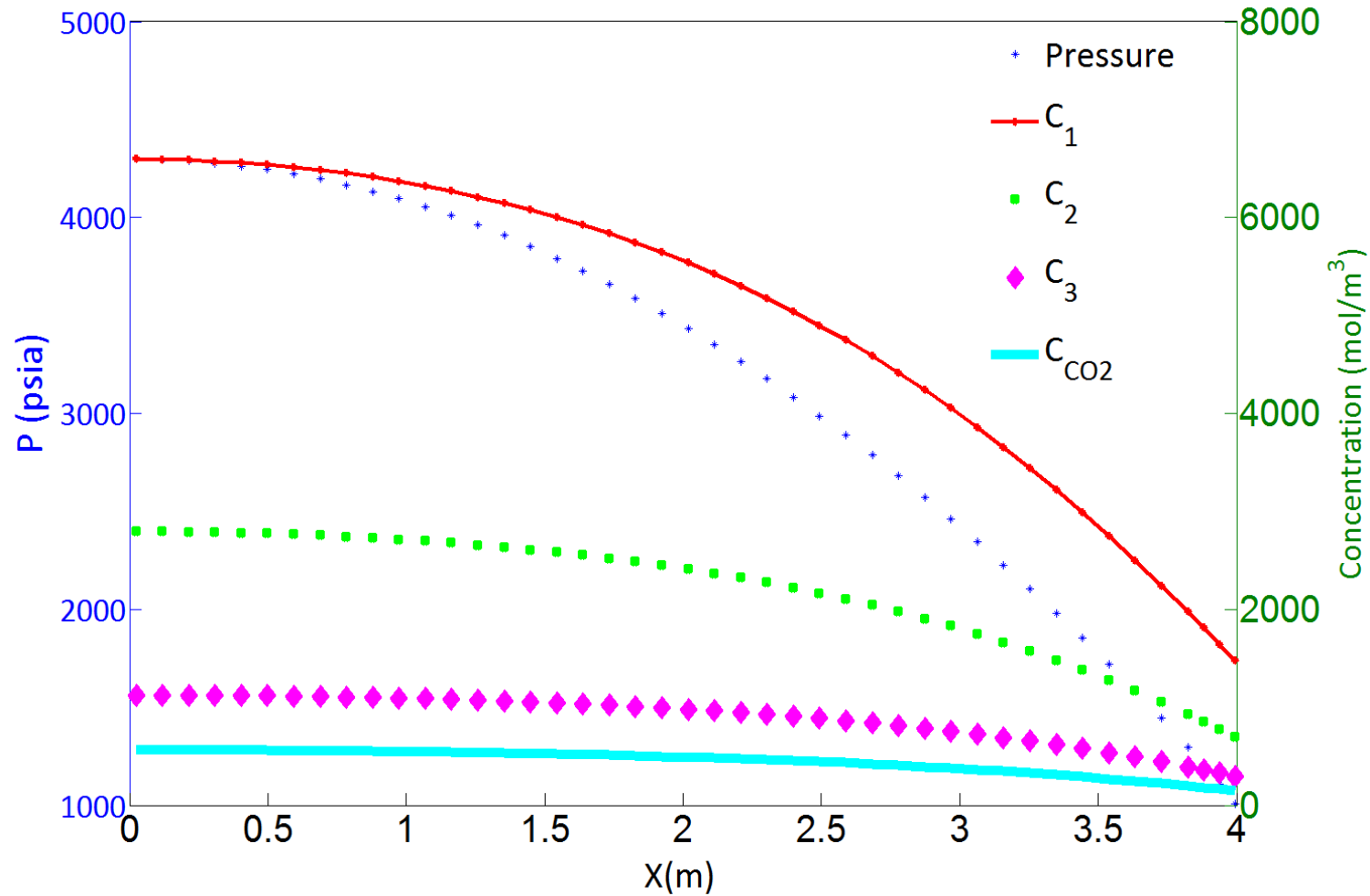
No flow bc at the inlet and Danckwertz bc at the outlet

$$[y_i]_{Outlet} = [y_i]_{N_{Block}} \quad \text{for } i = 1, \dots, N_c - 1$$

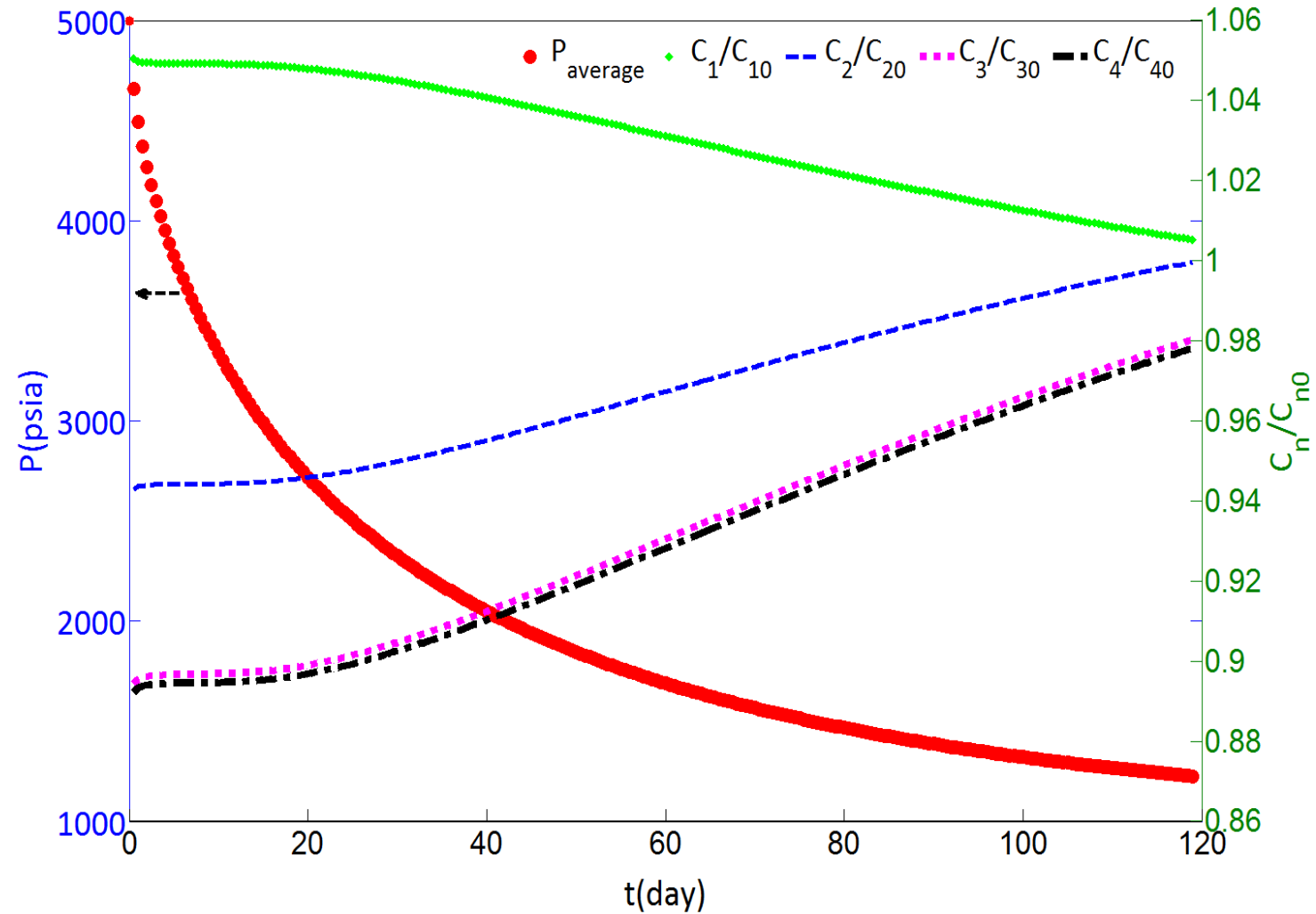
Input data

Property	Value
Darcy permeability, K_d (nD)	100
Porosity, ϕ	0.1
L(m)	4
Initial pressure (psi)	5000
Outlet pressure (psi)	1000
Temperature (K)	373
Tortuosity	4
Number of grid blocks (number of refined grid blocks near the outlet)	150 (70)

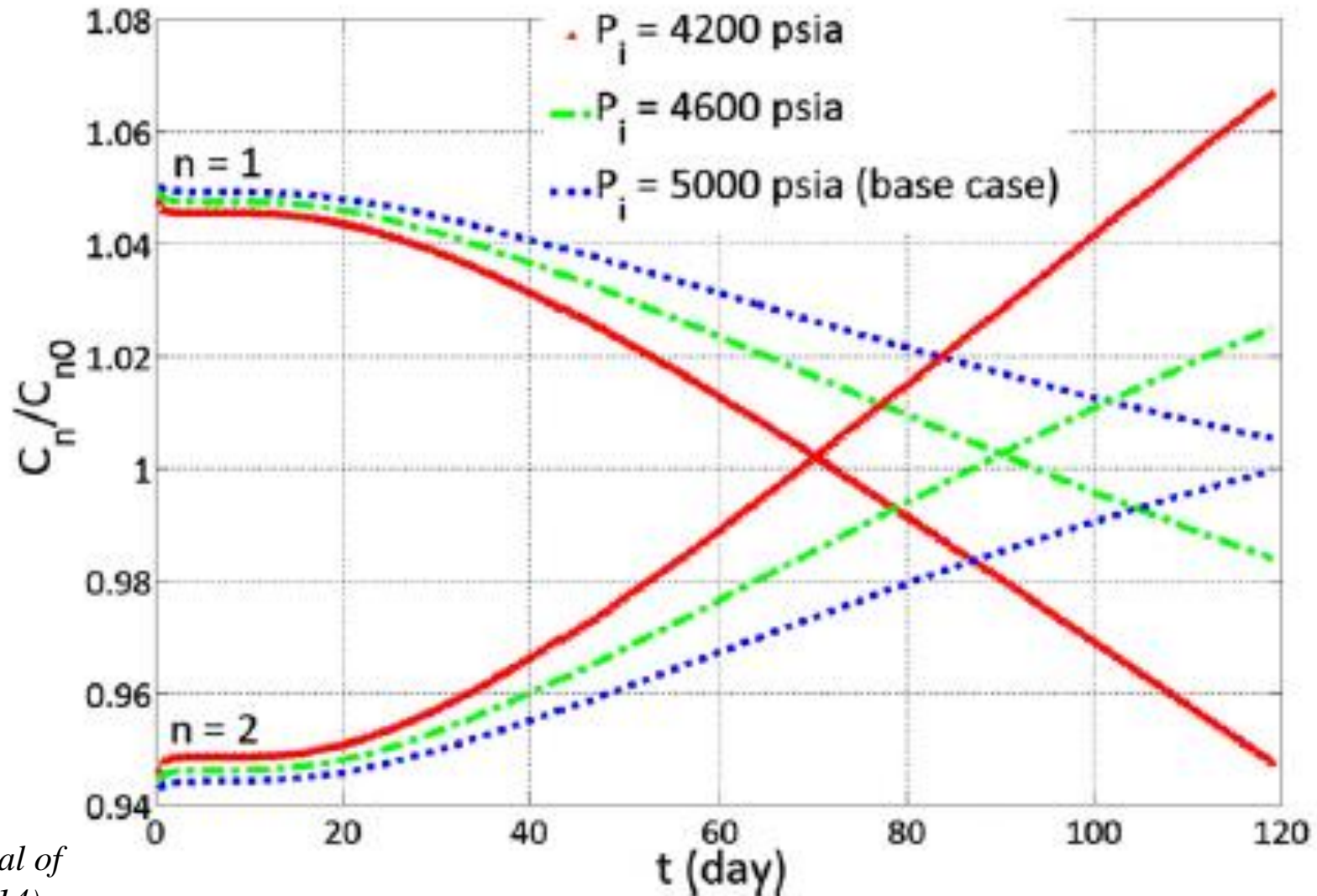
Spatial P & C profiles (12 days)



Temporal variation of P and normalized C_n

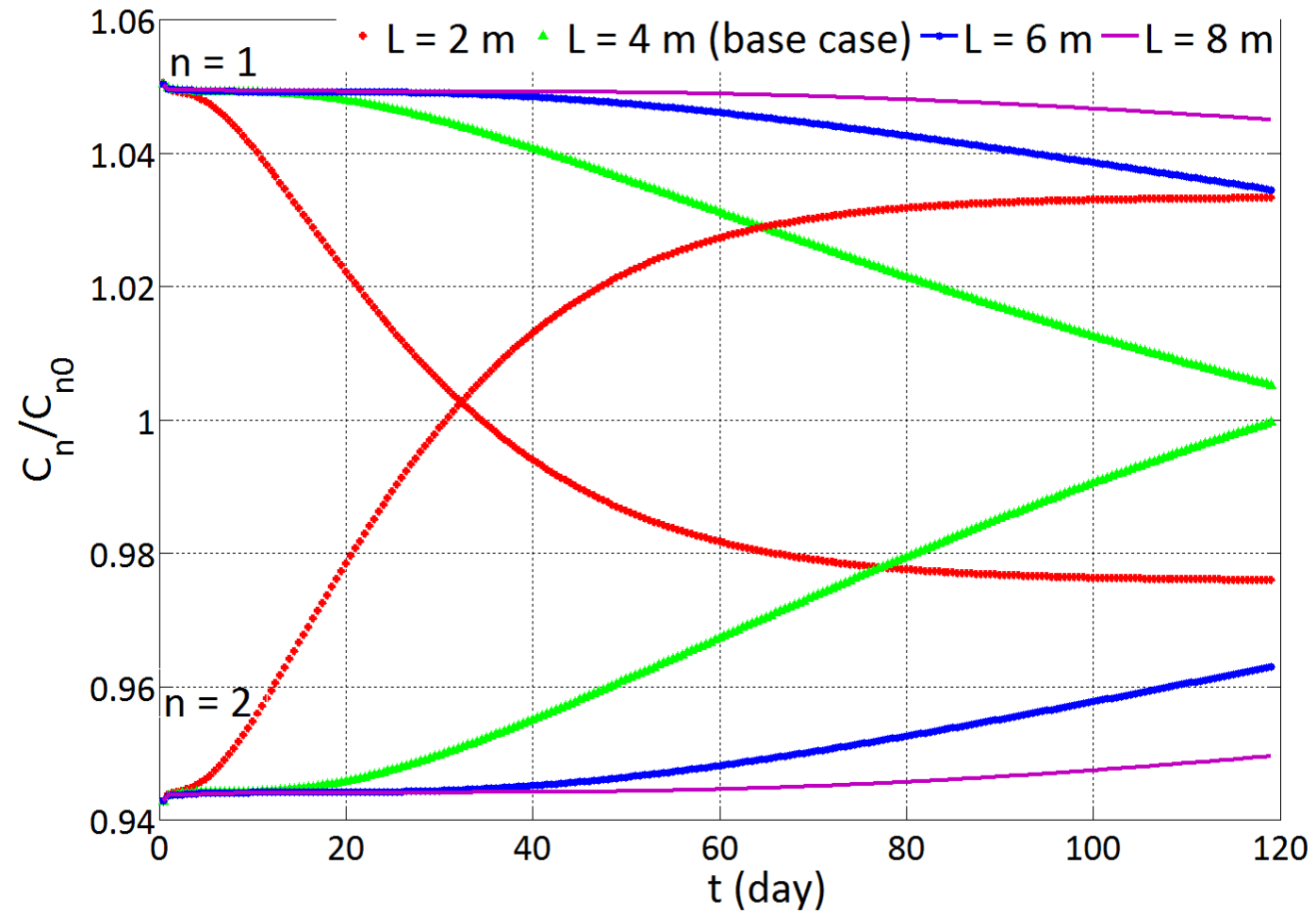


Effect of initial P



Rezaveisi et al.,
International Journal of
Coal Geology (2014)

Effect of matrix size



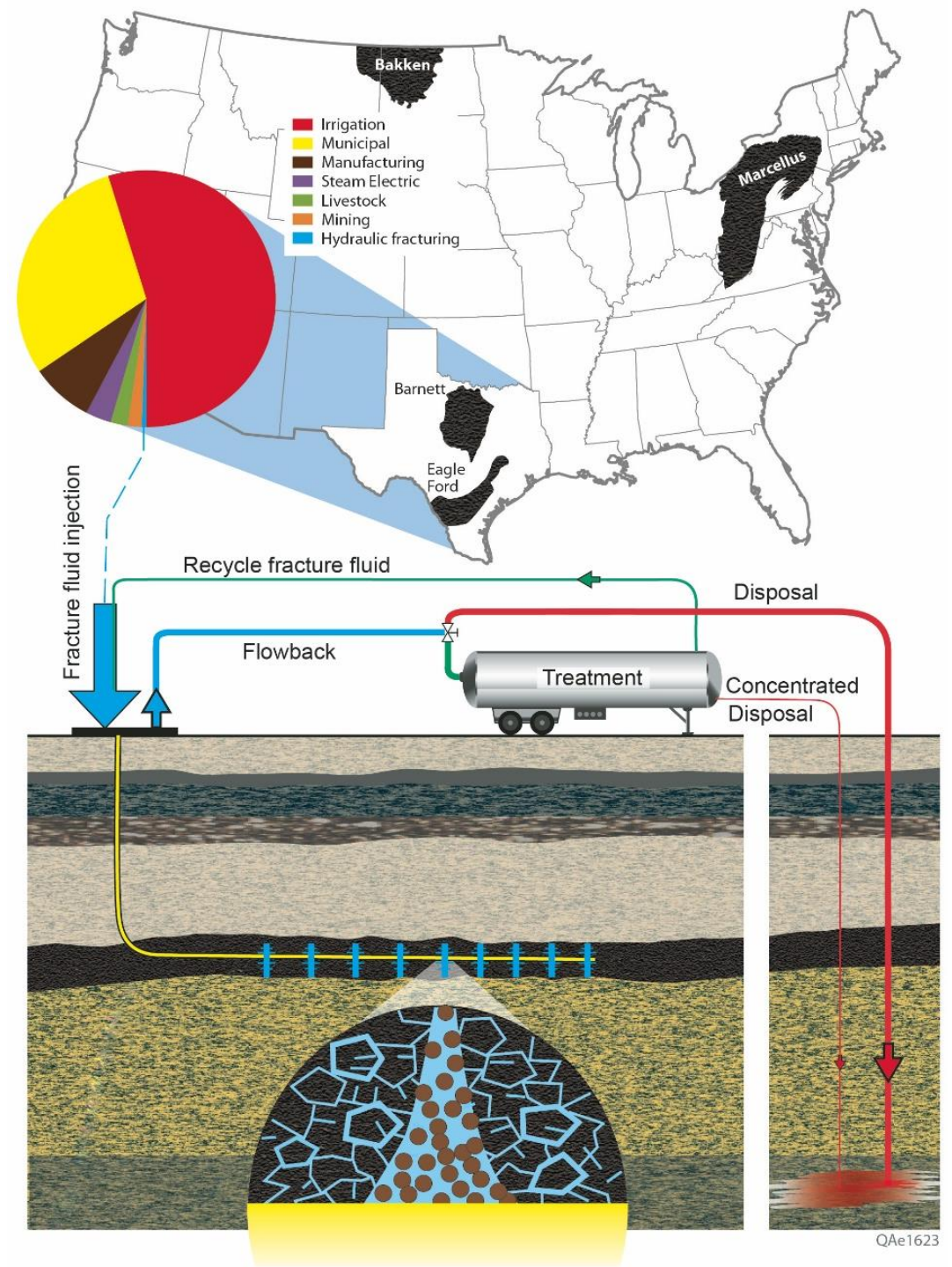
In a 2D model can be used to determine fracture spacing

Liquid flow in shale and fracture fluid loss

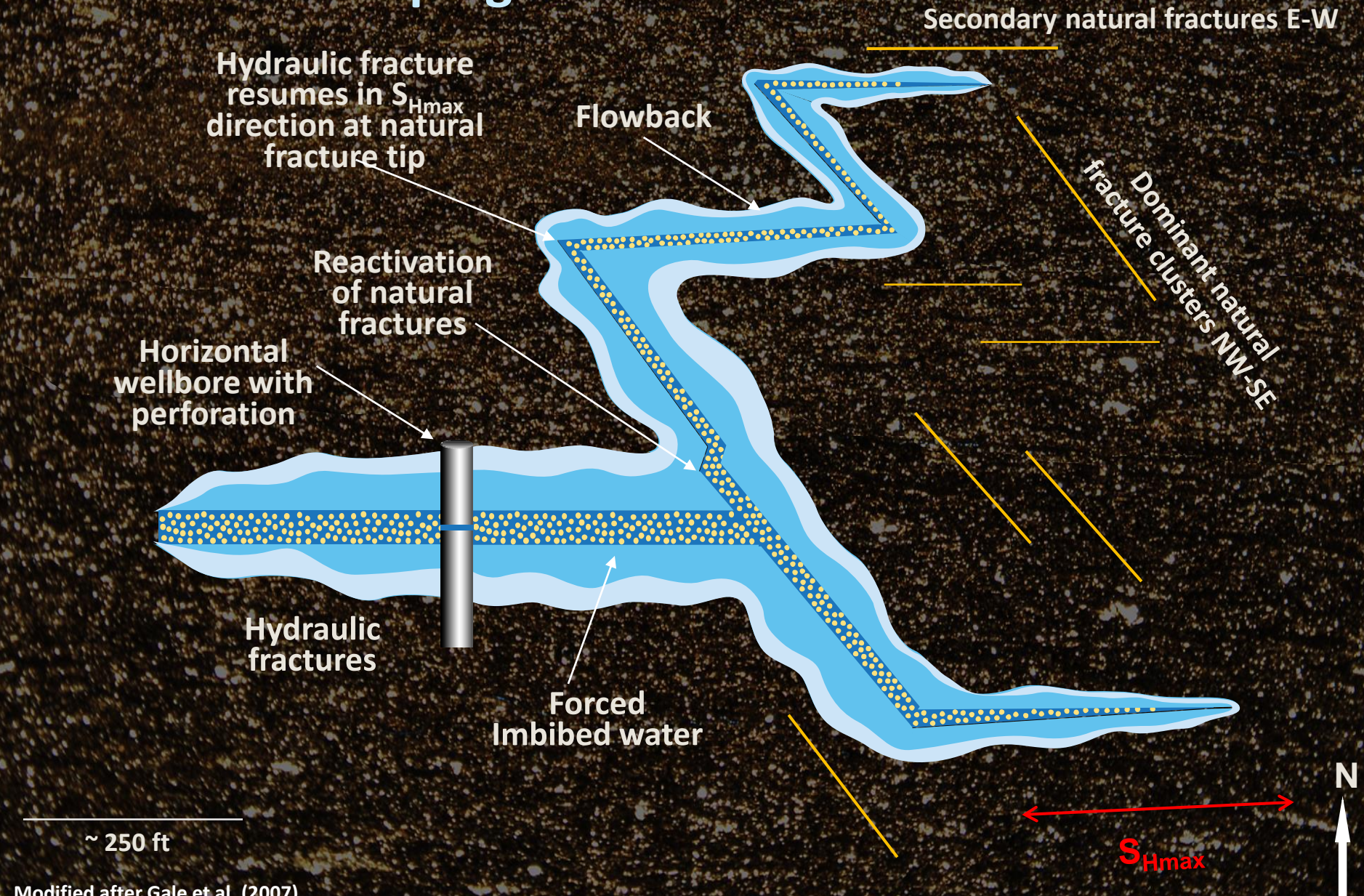
Hydraulic fracturing

After fracking, a portion of injected water

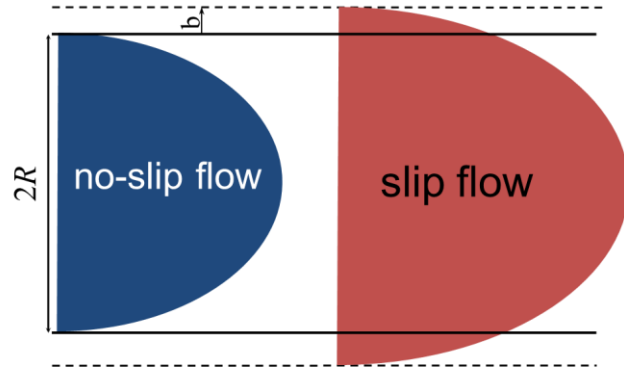
- flows back
- remains in fractures & gradually flows back
- leaks off into matrix



Hydraulic Fracture Treatments Pumping Phase

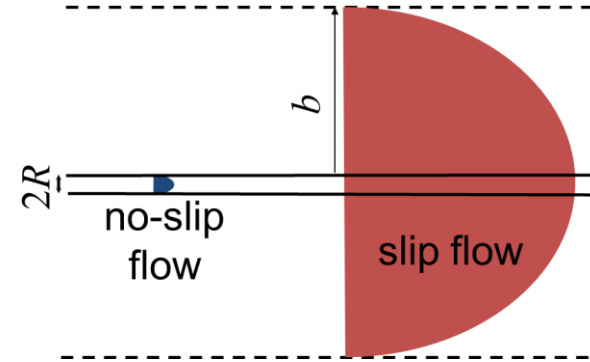


Liquid slip in a pore



$$R = 10 \mu\text{m}$$
$$U_{\text{slip}} = 1.02 U$$

**Negligible in
conventional reservoirs**



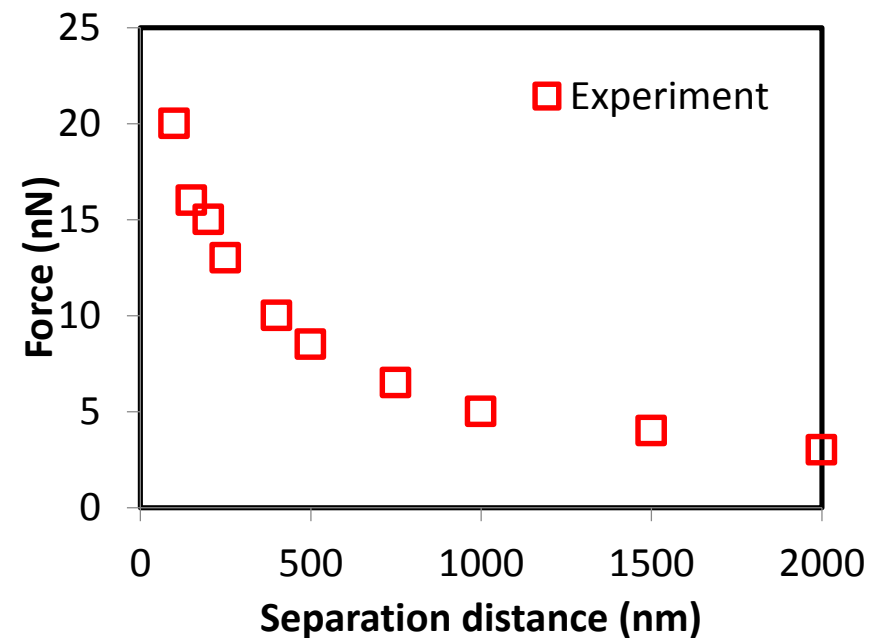
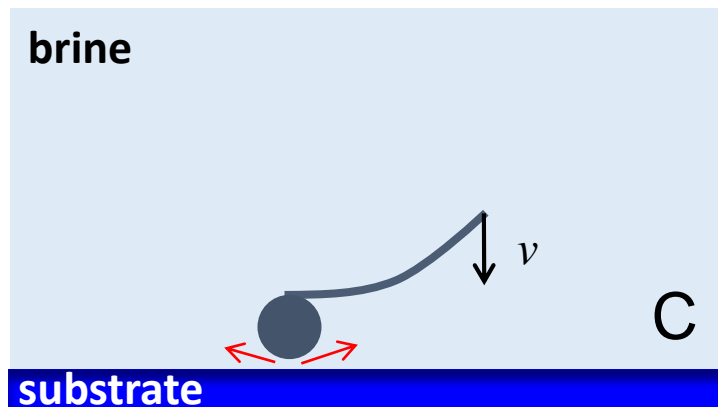
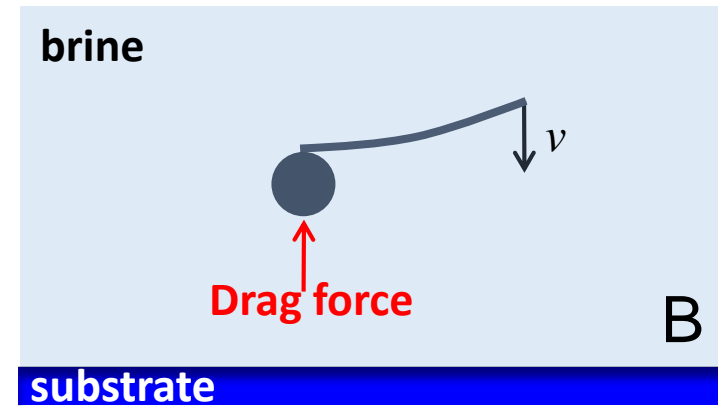
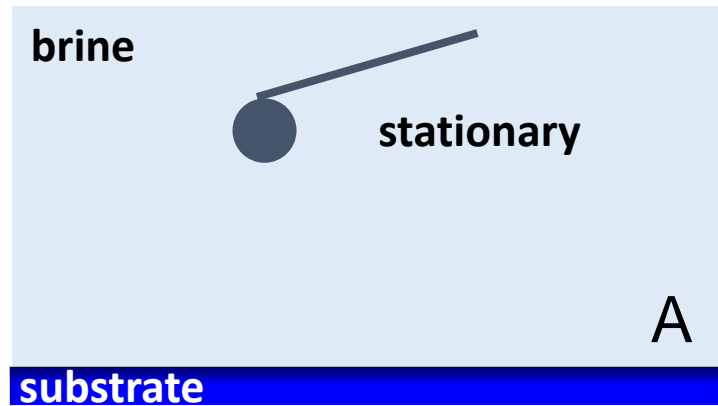
$$R = 10 \text{ nm}$$
$$U_{\text{slip}} = 10^2 U$$

**Slip must be included
in shale**

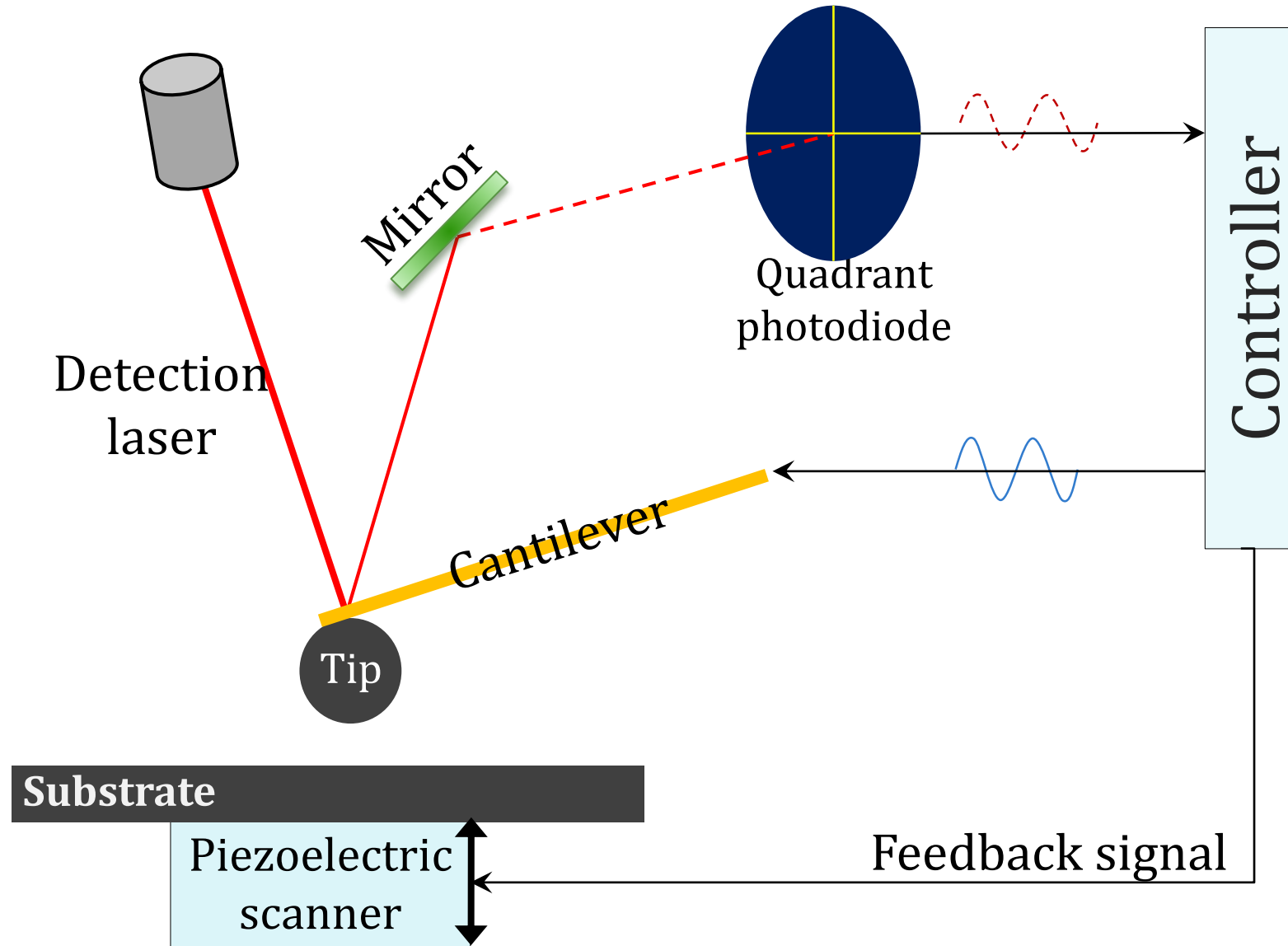
How to measure slip length?

- Slip depends on the surface and fluid type
- Slip length for a liquid flowing inside a tube or outside an object is the same
- It is easier to measure slip length for a fluid moving over an object
- We measure slip length over a spherical object and then relate it to liquid flow in pore

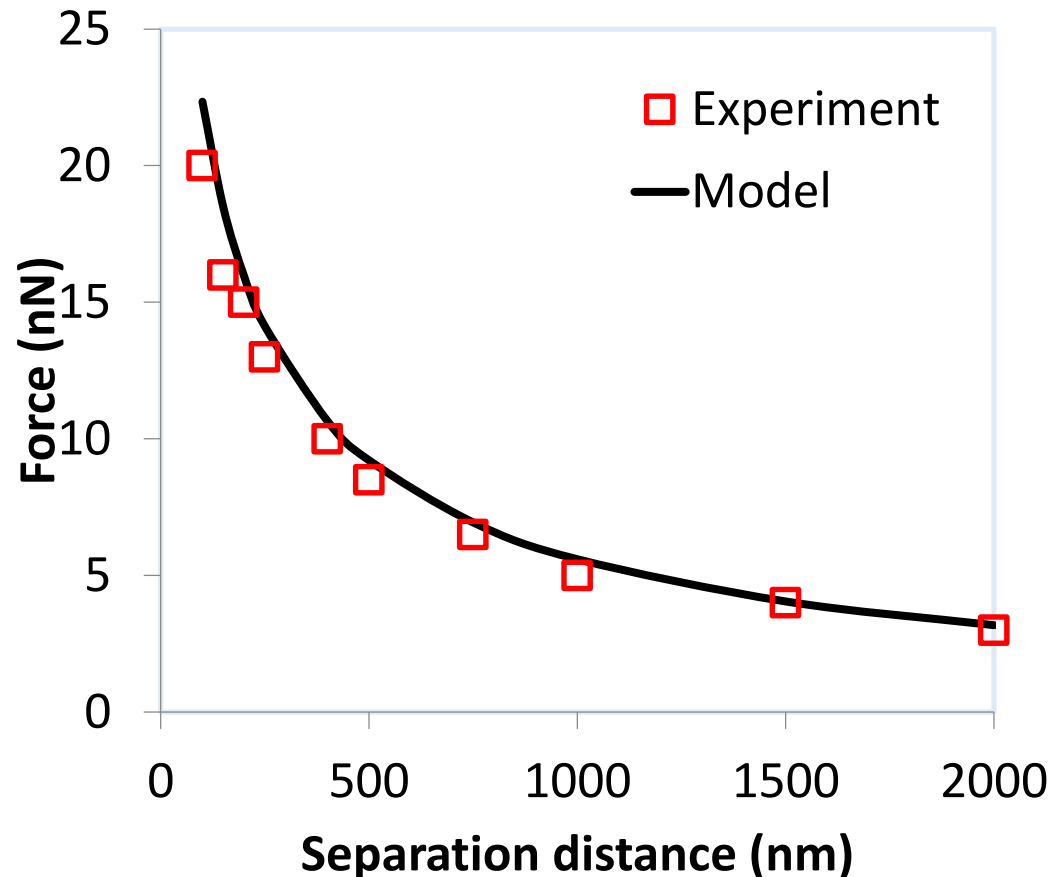
How to measure slip length?



Atomic force Microscopy (AFM)



Slip length from AFM data



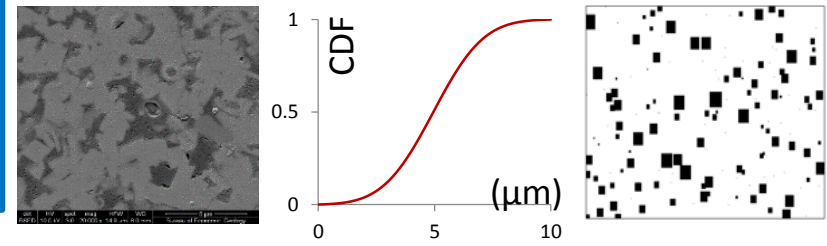
$$F = \frac{6\pi R^2 \mu v}{h} f^*$$

System of interest	Approach speed (μm/s)	
	20	15
CH-coated substrate and CH-coated sphere	280 nm n=182	253 nm n=190
Ion-milled shale and CH-coated sphere	189 nm n=369	176 nm n=353

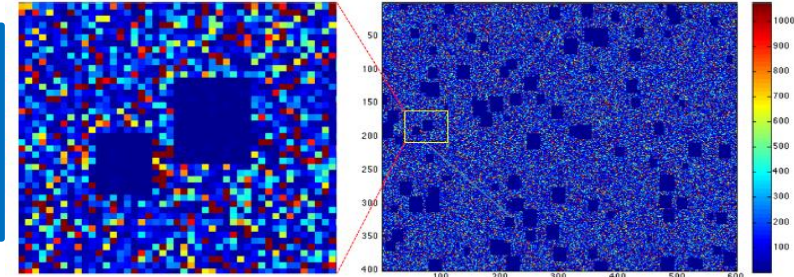
Javadpour et al., Fuel, 2015

Apparent liquid permeability model

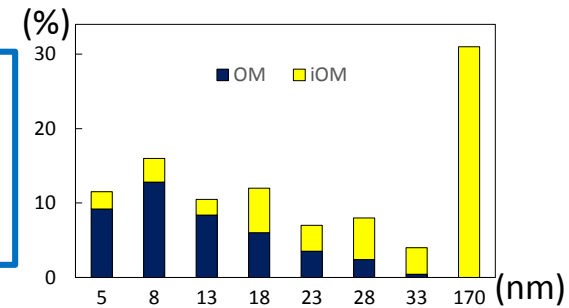
(a) Generate ensemble of OM & iOM realizations conditioned to OM Patch SD



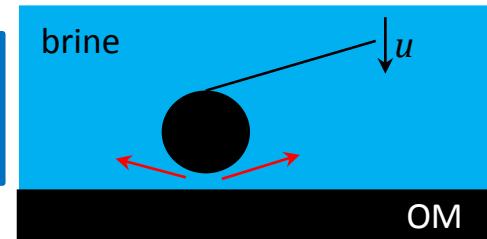
(b) Discretize space domain to gridblocks smaller than the smallest patch size



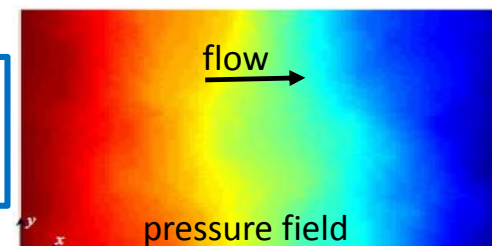
(c) Assign pore SD measured by N_2 sorption, MICP, or NMR within OM and iOM



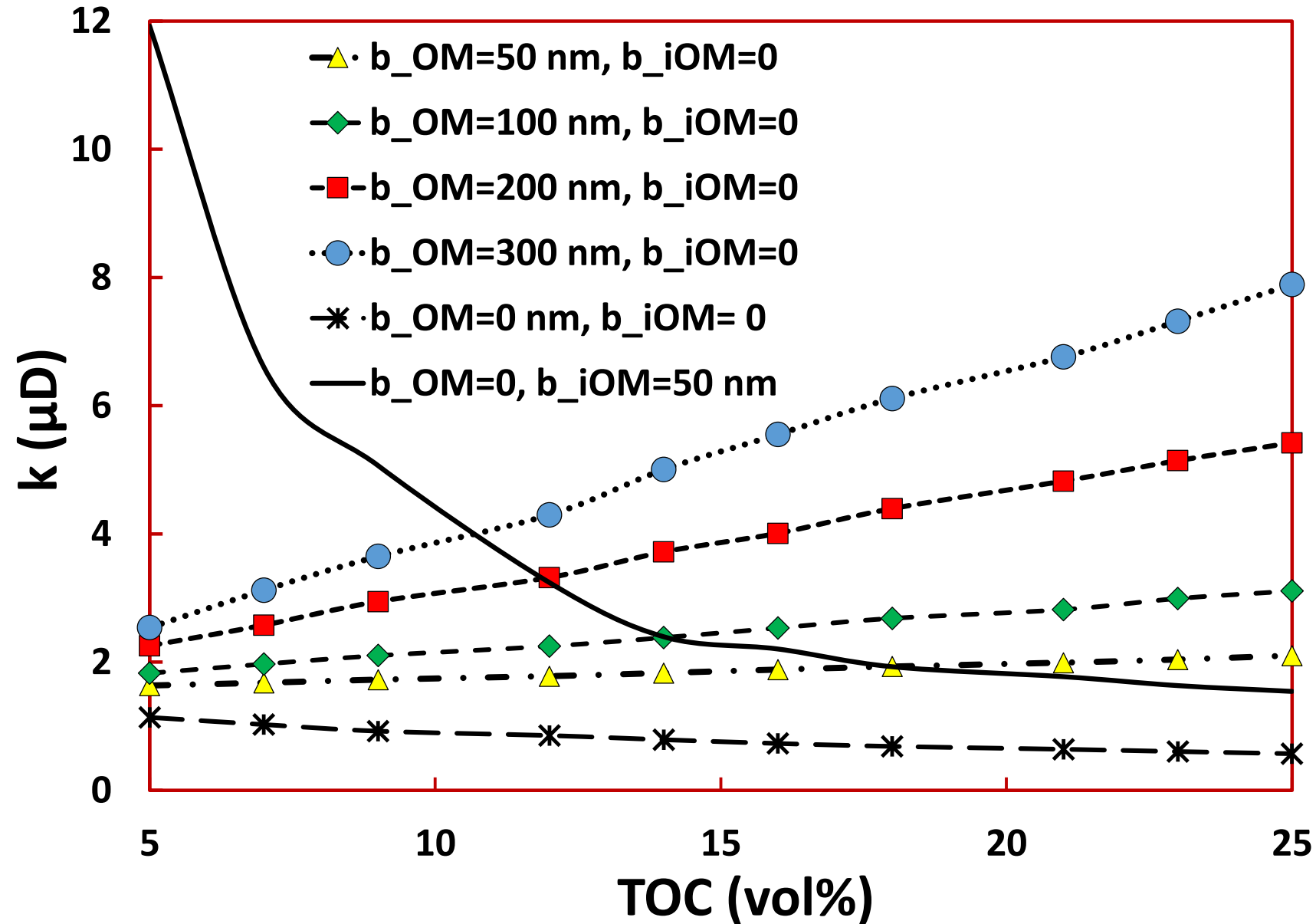
(d) Assign AFM measured slip length to pores in OM & iOM



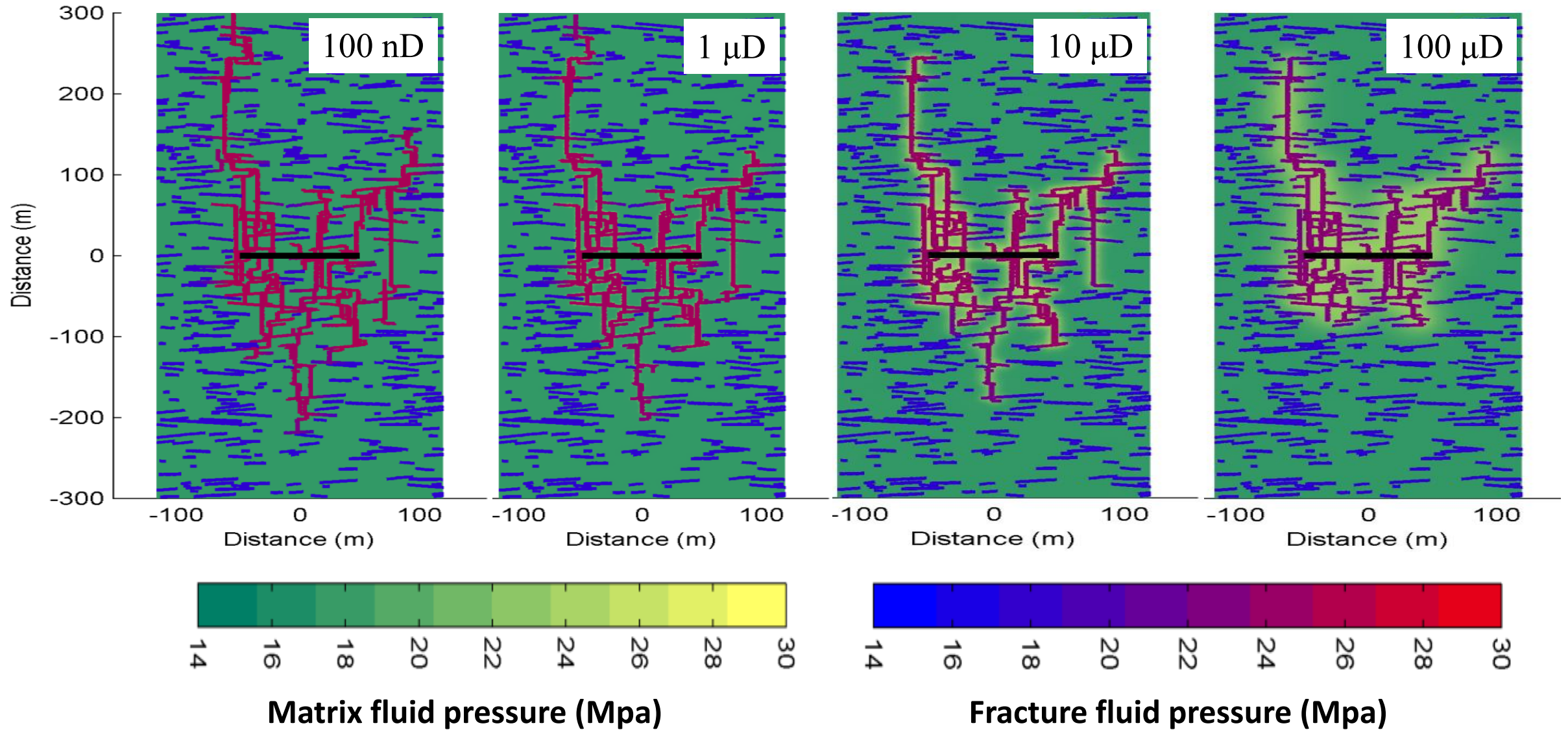
(e) Solve pressure field to calculate ALP or use Eq. (4)



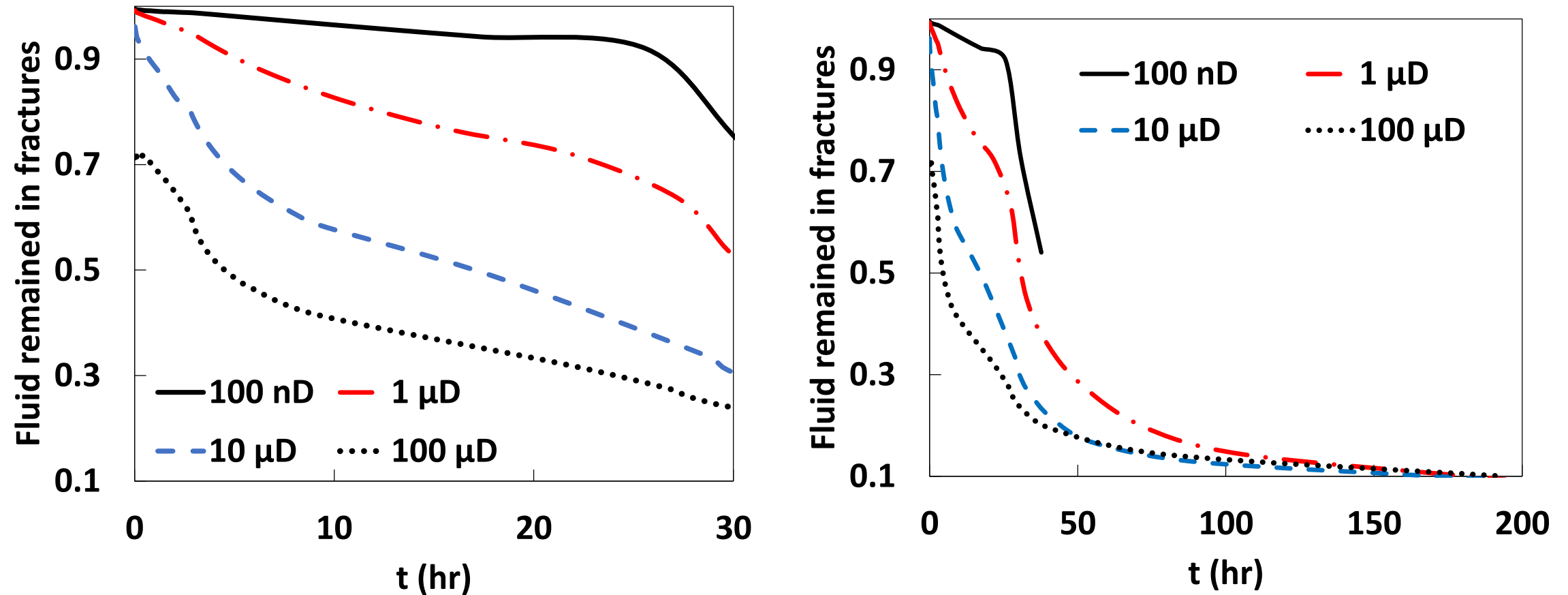
Impact of slip length & TOC on liquid permeability



Effect of liquid slip on fracturing



Liquid leak-off into matrix during fracturing



Javadpour et al., Fuel, 2015

Acknowledgments

- JSG, BEG, PGE, UT-Austin
- MSRL consortium, ConocoPhillips, Exxon
- Talented students and postdoctoral fellows
- Support staff and colleagues

Questions?